PET/MR Imaging in Head and Neck Cancer

Minerva Becker, MD[a,*], Claudio de Vito, MD[b], Nicolas Dulguerov, MD[c], Habib Zaidi, PhD[d,e,f,g]

KEYWORDS

• Head and neck cancer • Staging • PET/MR imaging • MR imaging • Diffusion-weighted imaging

KEY POINTS

- In patients with head and neck (HN) tumors, FDG PET/MR imaging shows a similar performance as PET/CT in terms of image quality, fusion quality, lesion conspicuity, anatomic location, and number of detected lesions.
- Studies investigating the T and N staging accuracy of PET/MR imaging compared with PET/CT in HN squamous cell carcinoma (HNSCC) have yielded conflicting results, nevertheless with a trend toward improved assessment of locoregional spread with PET/MR imaging. As most studies were based on small patient samples, larger studies are necessary to firmly establish the role of PET/MR imaging in this clinical setting.
- FDG PET/diffusion-weighted imaging (DWI) MR imaging with precisely defined diagnostic criteria including T2 signal and DWI characteristics yields excellent results for the detection of residual/recurrent HNSCC after radiotherapy with an excellent agreement between imaging-based and pathologic T stage.
- FDG PET/MR imaging has an excellent and similar diagnostic performance as FDG PET/CT for detecting distant metastases and distant second primary cancers in HNSCC patients; distant malignant lesions occur more often in the posttreatment surveillance group than in patients imaged for primary tumor staging.

INTRODUCTION

The rationale behind the integration of PET and MR imaging lies in the complementary strengths of each modality. PET provides metabolic information using radiotracers, whereas MR imaging offers detailed anatomic imaging with excellent soft tissue contrast, as well as functional information based on diffusion-weighted imaging (DWI), dynamic contrast-enhanced (DCE) perfusion imaging and magnetic resonance spectroscopy. By combining these modalities, PET/MR imaging can offer a comprehensive and synergistic qualitative and quantitative approach to better characterize tumors.

When hybrid PET/MR imaging technology was introduced in academic centers over a decade ago, the radiologic and nuclear medicine community had high expectations for oncologic head and neck (HN) imaging in terms of tumor characterization, localization and staging, detection of lymph nodes, distant metastases and recurrent disease,

[a] Diagnostic Department, Division of Radiology, Unit of Head and Neck and Maxillofacial Radiology, Geneva University Hospitals, University of Geneva, Rue Gabrielle-Perret-Gentil 4, Geneva 14 1211, Switzerland; [b] Diagnostic Department, Division of Clinical Pathology, Geneva University Hospitals, Rue Gabrielle-Perret-Gentil 4, Geneva 14 1211, Switzerland; [c] Department of Clinical Neurosciences, Clinic of Otorhinolaryngology, Head and Neck Surgery, Unit of Cervicofacial Surgery, Geneva University Hospitals, Rue Gabrielle-Perret-Gentil 4, Geneva 14 1211, Switzerland; [d] Diagnostic Department, Division of Nuclear Medicine and Molecular Imaging, Geneva University Hospitals, University of Geneva, Rue Gabrielle-Perret-Gentil 4, Geneva 14 1211, Switzerland; [e] Geneva University Neurocenter, University of Geneva, Geneva, Switzerland; [f] Department of Nuclear Medicine and Molecular Imaging, University of Groningen, University Medical Center Groningen, Groningen, Netherlands; [g] Department of Nuclear Medicine, University of Southern Denmark, Odense, Denmark
* Corresponding author.
E-mail address: Minerva.Becker@hcuge.ch

Magn Reson Imaging Clin N Am 31 (2023) 539–564
https://doi.org/10.1016/j.mric.2023.08.001

and tumor segmentation for radiotherapy planning.[1,2] Furthermore, imaging biomarkers extracted from PET/MR imaging, such as the apparent diffusion coefficient (ADC), maximum and mean standardized uptake values (SUV_{max}, SUV_{mean}), total lesion glycolysis (TLG), and vascular permeability constants (eg, volume transfer constant, K_{trans}), were shown to correlate with tumor grade and stage,[3,4] and in combination with clinical risk factors—they can predict the survival of HNSCC patients thus outperforming the traditional tumor node metastasis (TNM) system.[5]

Even if hybrid PET/MR imaging equipment is today not as widely available as stand-alone MR imaging and PET/CT technology, the research on combined PET and MR imaging information including DWI or perfusion imaging has led to an increasing understanding of HN cancer biology and to an improved diagnosis in challenging areas, for example, posttreatment evaluation.[6,7] Furthermore, combined PET and MR imaging information—whether derived from hybrid PET/MR imaging systems or from standalone MR imaging and PET/CT technology—is complementary and pitfalls of image interpretation can thus be avoided.[6–8] MR imaging can help to avoid FDG PET/CT pitfalls related to high physiologic FDG uptake of normal structures (eg, muscles, salivary glands) and it can also detect lesions with low FDG uptake (hypometabolic tumors, necrotic lymph nodes, or tumors located in vicinity of areas with high FDG metabolism), which can be missed on PET/CT[8] (**Fig. 1**). Vice versa, PET/CT can facilitate the detection of metastatic neck nodes and it can reveal neck carcinoma of unknown primary (NCUP), a more challenging task at MR imaging[9,10] (**Fig. 2**).

The primary aim of this review is to critically summarize the current literature on PET/MR imaging in HN cancer and to offer the interested reader a comprehensive appraisal of what has been achieved during the past decade while at the same time providing an outlook on future directions in the implementation and clinical use of multiparametric PET/MR imaging. The focus of this article is on HN squamous cell carcinoma (HNSCC).

HEAD AND NECK SQUAMOUS CELL CARCINOMA: IMAGING INDICATIONS AND PET/MR IMAGING PROTOCOLS

Squamous cell carcinoma (SCC) is the most common malignant tumor originating in the HN. It is the sixth most common tumor worldwide and its incidence is increasing with an anticipated rise by 30% by 2030.[11] Despite ongoing advances in radiotherapy, surgery, chemotherapy and immunotherapy, 5-year survival rates remain under 50%.[12] HNSCC arises either from the mucosal lining of the upper aerodigestive tract or from the skin. Tobacco and alcohol consumption are typically associated with SCC of the oral cavity, larynx, and hypopharynx.[11,13] In contrast, infection with the human papilloma virus (HPV)—mainly HPV-16—is typically associated with SCC of the oropharynx, whereas infection with the Epstein–Barr virus (EBV) is an important etiologic factor in SCC of the nasopharynx.[11] Finally, exposure to ultraviolet light plays an important role in the etiology of SCC of the skin and lip.

Staging of primary HNSCC of the upper aerodigestive tract includes clinical examination, panendoscopy, and cross-sectional imaging. Contrast-enhanced CT and MR imaging are the most commonly used cross-sectional imaging modalities to assess locoregional disease, and CT is also used to detect distant metastases or second primary tumors. Whether contrast-enhanced PET/CT should be used routinely for the initial HNSCC staging is still a matter of debate. However, in most institutions, PET/CT is recommended for the initial staging of locally advanced HNSCC (because of an increased risk of distant metastases) and in NCUP. Furthermore, PET/CT is also recommended for radiotherapy planning (see below).

For the follow-up of HNSCC patients, although PET/CT is routinely used in the posttreatment setting in different institutions, many institutions prefer MR imaging or CT for the locoregional assessment and an additional CT for the evaluation of the chest, whereas other institutions prefer to combine MR imaging and PET/CT or—if available—they perform PET/MR imaging. Irrespective of the imaging modality used, a baseline posttreatment surveillance study is carried out at 12 weeks after treatment, after which surveillance is done depending on local preferences given the paucity of literature demonstrating a clear benefit from surveillance imaging beyond the baseline posttreatment examination in asymptomatic patients.[14] However, in patients with a history of smoking, lung screening with chest CT is usually carried out during the first 2 to 5 years after treatment.

In clinical practice, most patients with HNSCC imaged with PET/MR imaging are selected by needing a dedicated HN MR imaging examination as well as whole body staging with PET.[15]

Imaging protocols for MR imaging and PET/MR imaging vary significantly from one institution to another. Nevertheless, a dedicated MR imaging examination of the HN region should include T1W, T2W, contrast-enhanced T1W sequences and a DWI acquisition. Some authors use fat-saturated T2W and fat-saturated post-contrast T1W images, whereas others do not recommend

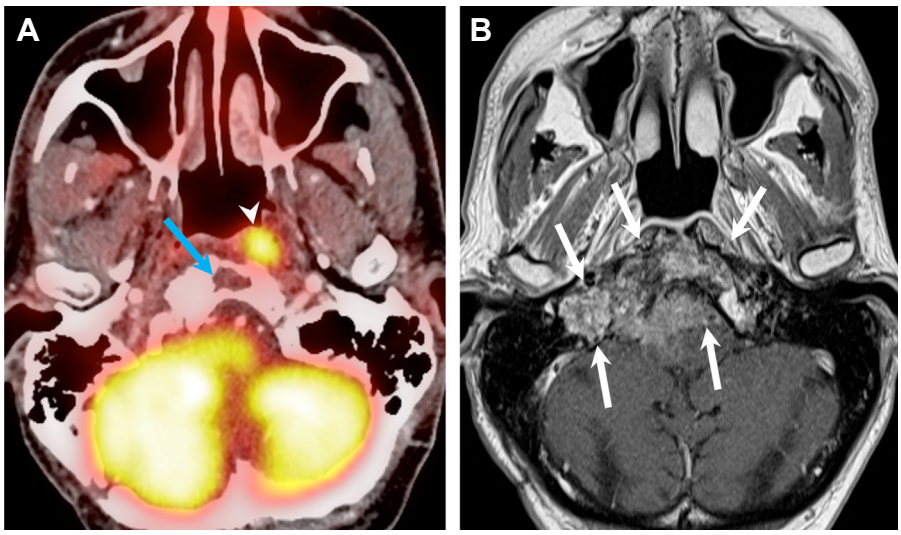

Fig. 1. (*A*) Axial PET/CT image shows asymmetric uptake behind the nasopharynx (*arrowhead*) and expected high uptake in the explored hindbrain. A lytic lesion in the clivus with well-defined sclerotic borders and without FDG uptake is also detected (*arrow*). The remaining of the total body PET/CT was normal. FDG uptake in the left longus colli muscle (*arrowhead*) was interpreted as physiologic. (*B*) Corresponding axial contrast-enhanced T1-weighted MR image obtained in the same patient illustrates an infiltrative, poorly delineated tumor invading the clivus, the right jugular fossa, the right petrous apex, and the brainstem (*arrows*), not revealed by PET/CT. Subsequent biopsy of the clivus, intracranially and of the nasopharynx showed a primary adenocarcinoma of the skull base. The increased FDG uptake in the left nasopharynx seen in A corresponds to tumor invasion of the longus colli muscle. Owing to intratumoral areas with variable FDG avidity and tumor vicinity to the highly metabolic brain parenchyma, this lesion is less well depicted by PET/CT than MR imaging. (*Reproduced from* Purohit et al.[8])

fat saturation.[13,16] An additional DCE perfusion imaging sequence is not recommended in clinical routine mainly because of a lack of consensus regarding relevant quantitative parameters.

PET/MR imaging examinations take longer than PET/CT examinations. Therefore, due to costs constraints and limited patient cooperation, different PET/MR imaging protocols for patients with HN cancer have been proposed; these protocols reflect institutional preferences for sequences and imaging planes.[17–19] Nevertheless, most investigators have proposed the sole acquisition of

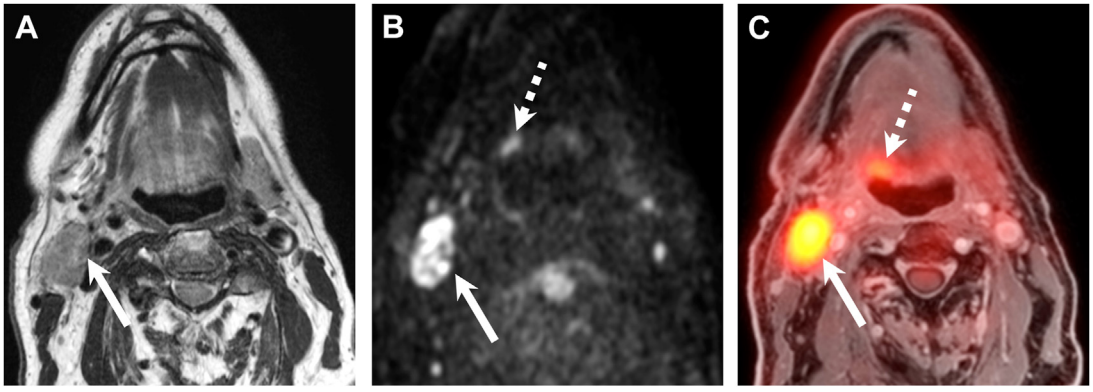

Fig. 2. Unknown primary cancer detected on PET/MR imaging. (*A*) T2W image shows a large level II lymph node metastasis (*arrow*) in a 63-year-old man. Ultrasonography-guided fine needle aspiration cytology revealed p16 positive squamous cell carcinoma (SCC). (*B*) Corresponding b1000 image from DWI. (*C*) FDG PET fused with the fat-saturated T1W contrast-enhanced image obtained at the same level. The metastatic lymph node (*arrows*) is equally well seen in (*A*, *B*) and (*C*). The small base of the tongue tumor is detected on DWI and PET (*dashed arrows*). Note, however, improved lesion conspicuity on PET due to increased FDG uptake. Endoscopic biopsy-confirmed HPV-positive SCC.

anatomic MR imaging sequences,[17,20–23] which can be used for PET attenuation correction and orientation (typically a Dixon-type T1W sequence ± intravenous (IV) contrast and a T2W sequence ± fat saturation in the HN and a Dixon-type T1W sequence or a periodically rotating overlapping parallel lines with enhanced reconstruction (PROPELLER) type sequence for the lung and abdomen), whereas only a minority of investigators has proposed a full diagnostic HN MR imaging protocol including DWI ± DCE perfusion imaging followed by anatomic MR imaging sequences for the chest, abdomen, and pelvis.[6,18,24] Using the MR imaging part of PET/MR imaging mainly for anatomic imaging makes sense given the superior soft tissue discrimination of MR imaging in comparison to CT, especially in the HN. However, if MR imaging is only employed for anatomic orientation, the full potential of PET/MR imaging is not used.[25]

DETECTION OF FOCAL LESIONS AND QUANTIFICATION ON PET/MR IMAGING

Most early publications on PET/MR imaging in HN cancer have focused on lesion detection and quantification in comparison to PET/CT.[19,26–29] Based on these publications, the following conclusions can be drawn.

- In patients with HN tumors, PET/MR imaging shows a similar performance to PET/CT in terms of image quality, fusion quality, lesion conspicuity or anatomic location, number of detected lesions, and number of patients with and without malignant lesions.
- There is an excellent correlation for SUV measurements on both modalities, nevertheless SUVs measured in malignant lesions, benign lesions, and organs on PET/MR imaging are underestimated compared with PET/CT.
- Differences in SUVs can be partly attributed to what kind of MR imaging-based attenuation correction map was used and partly to tracer kinetics, as PET/MR imaging and PET/CT were performed sequentially after administration of a single [18F] Fluorodeoxyglucose dose.
- Intra- and interobserver agreement for ADC and SUV measurements is very good.

CORRELATION BETWEEN PET/MR IMAGING-DERIVED BIOMARKERS

HNSCC typically have an increased FDG uptake, which reflects their increased glucose metabolism and they display restricted diffusivity at DWI, which corresponds to increased cellularity, lower ADC values depicting higher tumor cellularity. ADC values show a significant correlation with tumor differentiation, a higher grade tumor showing more restriction than a lower grade tumor.[30,31]

Several investigators have evaluated the correlation between quantitative FDG PET parameters and ADC values to find out whether there is a correlation between metabolic tumor activity (SUV_{max}, SUV_{mean}, TLG) and tumor cellularity (ADC values). Based on studies including 35 to 71 HNSCC patients, most investigators found that quantitative FDG uptake parameters were not significantly correlated with ADC values; therefore, the two parameters are most likely independent imaging biomarkers with the potential to provide complementary information on microstructural characteristics and biological behavior of HNSCC.[30–36] Nevertheless, Nakajo and colleagues reported a significant inverse correlation between SUV and ADC values in a series of 26 HNSCC patients.[37] Likewise, Han and colleagues reported a significant inverse correlation between ADC_{min} and TLG in 34 patients. However, the reported correlations were moderate to low with correlation coefficients varying between −0.56 and −0.35, respectively.[37,38] Moreover, several investigators have reported significant correlations between perfusion parameters (K_{trans}, K_{ep}, V_e) and PET parameters on the one hand, and between perfusion parameters and DWI parameters on the other hand.[3,31,38]

In conclusion, the relationships between DWI, FDG PET and DCE perfusion parameters rather suggest complex interactions and the reported data cannot be considered as evident with the exception of a most likely absent correlation between metabolism and cellularity in HNSCC. Nevertheless, if we expect to apply deep learning (DL) models for precise tumor segmentation and evaluation of prognostic factors further studies on larger patient cohorts are mandatory.

STAGING OF PRIMARY HEAD AND NECK SQUAMOUS CELL CARCINOMA

Local Tumor Evaluation (T Staging)

In primary HNSCC, tumor size, thickness and depth of invasion are directly correlated with tumor aggressiveness.[12] Correctly evaluating deep tumor spread and T stage in HNSCC has direct implications for treatment planning and prognosis.

Both primary and recurrent HNSCC have characteristic PET/DWI MR imaging features, which include an intermediate signal intensity on T1W, T2W, or fat-saturated T2W sequences, moderate enhancement after intravenous (IV) administration of contrast material, restricted diffusivity with ADC values less than 1.2 to 1.3 $\times$ 10^{-3} mm^2/s,

and increased FDG uptake with SUV_{max} values usually greater than 3 (Fig. 3).

To validate PET/MR imaging findings, correlation with cross-sectional whole-organ histologic slices is the ideal approach (Fig. 4). However, this is quite difficult to achieve in a busy clinical setting and because many patients do not undergo surgery. Most studies evaluating the diagnostic performance of FDG PET/MR imaging for local tumor staging of primary HNSCC are based on small sample sizes.[39–41] Moreover, not all authors precisely specify the standard of reference, and functional MR imaging sequences were not used. Also, some studies compared PET/MR imaging with PET/CT results, whereas other studies lacked comparative data with PET/CT.

Among these studies, Schaarschmidt and colleagues found no significant difference in T and N staging among PET/MR imaging, PET/CT, and MR imaging alone in 12 patients with primary HNSCC, histopathology of the resected tumors serving as the standard of reference.[39] In a study including 20 patients with hypopharyngeal SCC (with histopathology of the surgical specimen in 11 patients), Huang and colleagues found that the T staging accuracy of PET/MR imaging, PET/CT, and MR imaging alone was similar, that is, 82%, 64%, and 73%, respectively.[40] Sekine and colleagues compared the diagnostic accuracy of PET/MR imaging and PET/CT for the initial staging of 27 patients with newly diagnosed HNSCC and reported a comparable TNM staging accuracy with both modalities, although there was a trend toward higher sensitivity and specificity with PET/MR imaging.[41] In contrast, Samolyk-Kogaczewska and colleagues reported a superior T staging accuracy with PET/MR imaging in comparison to CT in 21 patients with HNSCC.[42] In a retrospective study including 36 patients with oropharyngeal SCC, Flygare and colleagues found no significant differences in T staging or in measurement of maximum tumor diameter between PET/DWIMR imaging and

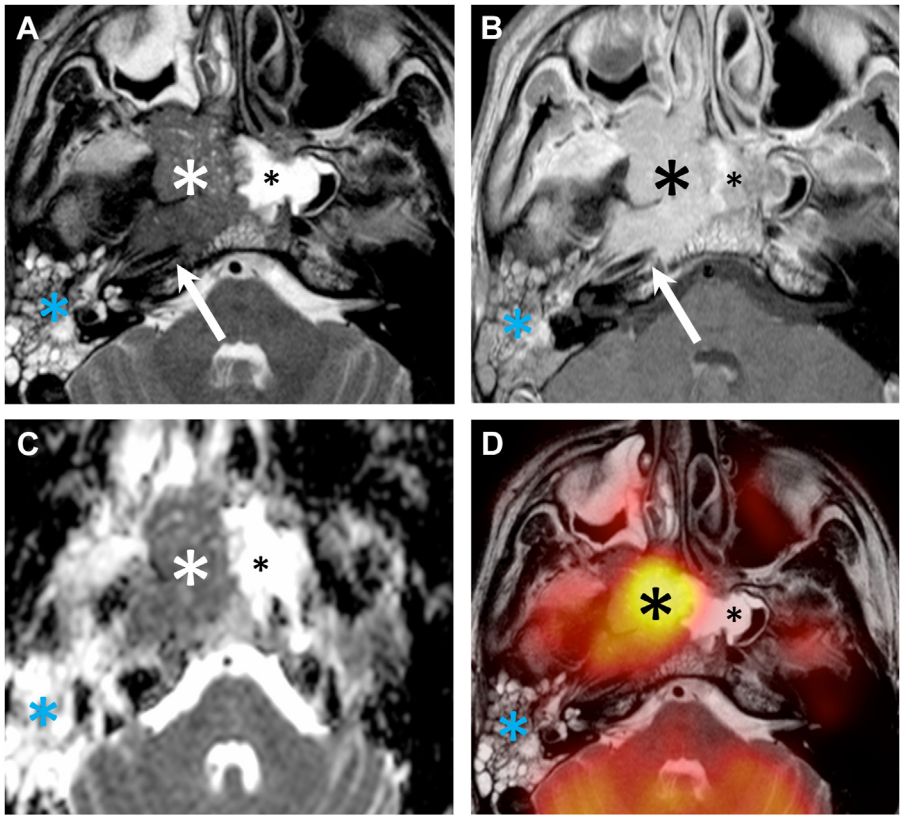

Fig. 3. Characteristic PET/DWIMR imaging features of an advanced primary nasopharyngeal cancer. (*A*) T2W image. (*B*) Contrast-enhanced T1W image. (*C*) ADC map from DWI. (*D*) Fused PET and T2W image. Infiltrating tumor (*large asterisks*) with an intermediate signal intensity on T2W images, enhancement after IV administration of contrast-material and restricted diffusion (ADC = 0.86×10^{-3} mm^2/s). High FDG uptake (SUV_{max} = 11). Skull base invasion reaching the right carotid canal (*arrows*). Blue asterisks indicate fluid retention in the right mastoid air cells. Small asterisks indicate fluid retention in the sphenoid sinus.

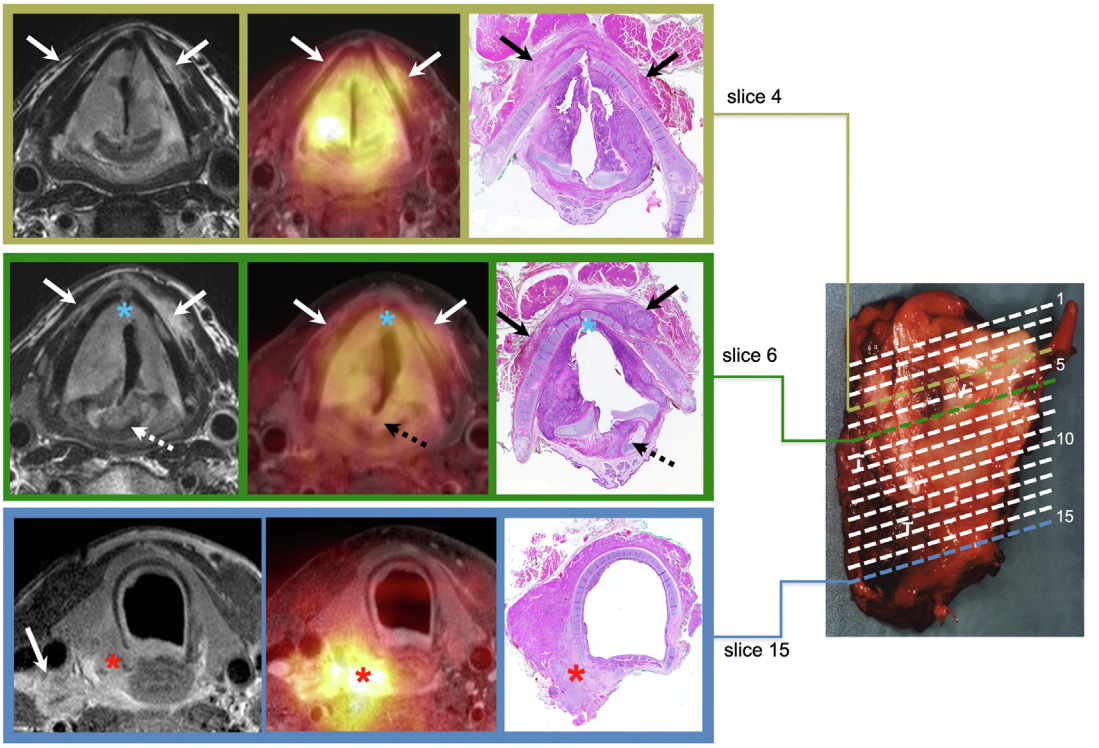

Fig. 4. Radiologic -pathologic correlation protocol enabling precise slice by slice correlation between MR imaging, PET, and whole-organ serial histology. Contrast-enhanced T1W images: left column. Fused PET and contrast-enhanced Dixon sequence: middle column. Whole-organ serial histology: right column. After surgical resection, whole-organ slices are obtained parallel to the imaging plane every 3 mm. Selected slices are shown. Slice 4: supraglottic larynx. Slice 6: glottic larynx. Slice 15: cervical trachea. In this figure with a bilateral transglottic SCC of the larynx, there is invasion of the anterior (*blue asterisks*) and posterior commissure (*dashed arrows*), paraglottic space bilaterally and there is tumor spread into the strap muscles (arrows in slice 4 and 6). The tumor has invaded the tracheoesophageal groove (red asterisks on slice 15). Metastatic lymph with extranodal spread is also seen on the contrast-enhanced T1W image at the level of the trachea (*arrow on slice 15)*. Note variation in SUV values with locally higher values on slice 4 and 15.

PET/CT; the standard of reference for the T stage was, however, not specified.[43] In the study of Flygare and colleagues, the interobserver agreement between two readers was higher for PET/DWIMR imaging than for PET/CT. However, there was only a weak agreement between PET/CT and PET/DWIMR imaging for the T stage.[43] In a prospective study including 113 patients with nasopharyngeal carcinoma, Chan and colleagues reported that PET/MR imaging was more accurate than MR imaging and PET/CT for the staging of nasopharyngeal cancer, however, the investigators did not report any *P* values for pairwise comparisons; for the assessment of deep submucosal tumor spread, MR imaging served as the standard of reference.[44] Kuhn and colleagues found slight advantages of PET/MR imaging over PET/CT for the local assessment of HNSCC, especially for invasion of adjacent structures and PNS; however, the standard of reference for deep tumor spread was not specified.[45] The investigators also reported that tumors in the oral cavity and oropharynx were more often affected by artifacts on PET/CT (because of dental hardware), whereas tumors in the hypopharynx and larynx were affected more often by artifacts on PET/MR imaging (because of breathing and swallowing) (**Fig. 5**). In a cohort of 35 patients with nasopharyngeal carcinoma, Cheng and colleagues reported that T2W and non-enhanced T1W PET/MR imaging were superior to PET/CT for the visualization of primary lesions due to higher lesion conspicuity.[36]

Other studies focused on the local assessment of HNSCC and on whether MR imaging and/or PET parameters could predict local tumor resectability. Among these studies, Meerwein and colleagues evaluated tumor fixation to the prevertebral space in 59 patients with advanced SCC of the hypopharynx.[46] Neoplastic invasion of the prevertebral space renders a tumor unresectable;

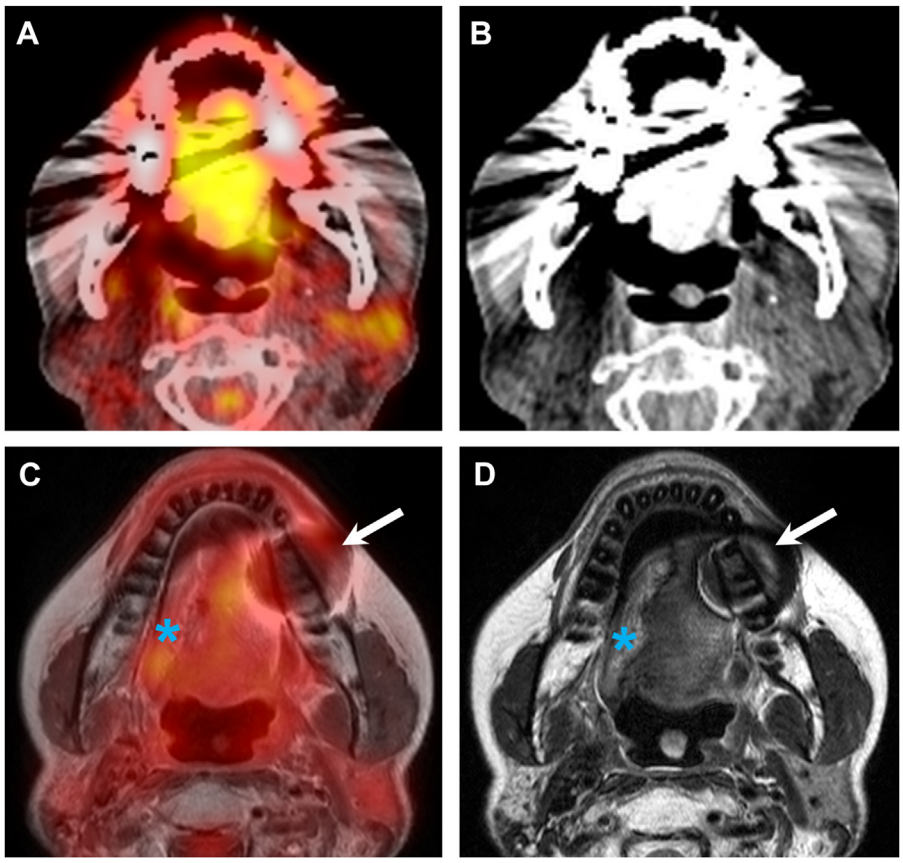

Fig. 5. (*A, B*) FDG PET/CT images. (*C, D*) Corresponding PET/MR imaging obtained in the same patient after surgery and radiotherapy for SCC of the oral cavity. Owing to dental hardware, the oral cavity can be hardly evaluated on PET/CT; however, on PET/MR imaging, no recurrent disease can be identified. Note the relatively limited artifact due to metal implant on the left (*arrows*). Normal flap used to reconstruct the floor of the mouth on the right (*asterisks*).

prevertebral space invasion can be diagnosed by exploratory cervicotomy or by palpation during panendoscopy. Both the MR imaging feature "complete obliteration of the retropharyngeal fat" and the combination of PET-based parameters "focal FDG uptake of prevertebral muscles and increased SUV_{max} of the primary tumor" independently predicted fixation to the prevertebral space with an accuracy of 98%.[46] In a series of 58 patients with primary and recurrent HNSCC, Sekine and colleagues evaluated further factors affecting local tumor resectability (eg, invasion of the mediastinum, mandible and laryngeal cartilages, or perineural spread [PNS]) and found that both contrast-enhanced PET/CT and PET/MR imaging with a fully diagnostic regional MR imaging protocol (but without DWI or perfusion imaging) performed equally well, although there was a slight but nonsignificant trend toward more accurate results with PET/MR imaging.[47] The standard of reference in this study consisted in clinical findings, intraoperative results and/or histopathology, which was, however, available only in 51% of cases.

PNS along the cranial nerves has a major impact on prognosis, risk stratification, staging, and treatment planning in a variety of HN tumors; however, it is often underdiagnosed clinically. HNSCC and adenoid cystic carcinoma have the highest incidence of PNS, followed by desmoplastic melanoma, mucoepidermoid carcinoma, and lymphoma.[48,49] Contrast-enhanced MR imaging is considered the most appropriate imaging modality to detect PNS and invasion of the skull base.[50] Primary MR imaging findings in PNS include thickening, nodularity, nerve enhancement, and fat pad obliteration, and secondary MR imaging findings are denervation of muscles as well as changes of the superficial muscular aponeurotic system.[50] PNS can also be detected on FDG PET—if tumors are FDG avid or in the presence of extensive PNS—and correlation with anatomic

imaging improves the assessment of PNS presence and extent and skull base invasion.[49,51] Although some investigators highly recommend FDG PET/CT to assess PNS, others suggest using PET/MR imaging or PET/CT only as problem-solving tools in posttreatment surveillance as MR imaging has a high diagnostic performance in the assessment of PNS.[50,52] As suggested by several investigators and based on our own experience, PNS lesions can be missed on PET/CT scans and combining PET with MR imaging improves the detection of PNS (**Fig. 6**).[44,47,51] Nevertheless, there are currently no studies comparing the diagnostic performance of PET/MR imaging with PET/CT or MR imaging alone specifically addressing PNS, and further research is necessary to establish more conclusive comparisons.

Lymph Node Evaluation (N Staging)

The presence of lymph node metastases in HNSCC is one of the most important parameters affecting prognosis, one single positive node already decreasing survival by 50%.[53] Other factors affecting survival include the number of metastatic nodes, their location in the neck (upper vs lower neck), and the presence of extranodal extension (ie, cancer extending beyond the nodal capsule). Therefore, early detection and accurate staging of lymph node metastases are crucial for determining appropriate treatment strategies to improve patient outcome.

To diagnose metastatic lymph nodes in HNSCC, the following PET/DWI/MR imaging criteria are applied (**Figs. 7** and **8**): morphologic MR imaging criteria (size > 10 mm, rounded shape, irregular margins, inhomogeneous enhancement, central nodal necrosis); restricted diffusivity (ADC values in metastatic nodes are lower than in reactive nodes; however, no uniform cutoff value is available in the literature); and increased glucose metabolism (focal FDG uptake of metastatic nodes, but no uniform cutoff value, occasionally absent FDG uptake in entirely necrotic nodes).

Most studies evaluating the diagnostic performance of FDG PET/MR imaging for the N staging of HNSCC are either based on relatively small sample sizes or there is no histopathologic correlation to confirm the N stage. Among the few studies with neck dissection specimen as standard of reference, a comparable N staging accuracy with PET/MR imaging and PET/CT was reported by Sekine and colleagues in 14 HNSCC patients, by Schaarschmidt and colleagues in 25 HNSCC patients, and by Huang and colleagues in 11 patients with hypopharyngeal SCC, respectively.[39,40,41] Huang and colleagues also reported that PET/MR imaging, PET/CT, and MR imaging alone had a

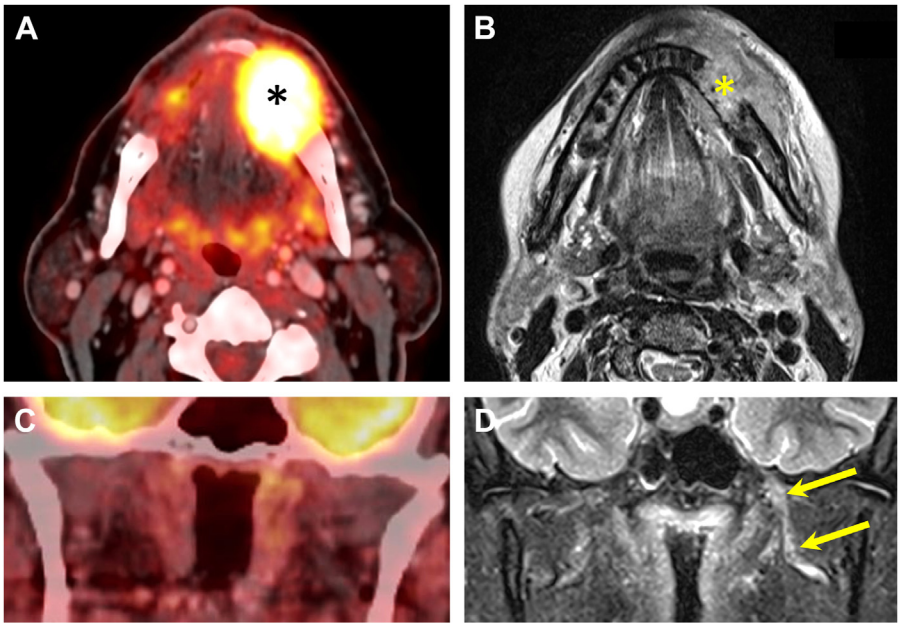

Fig. 6. (*A, C*) PET/CT images. (*B, D*) Corresponding MR imaging obtained in the same patient with SCC of the oral cavity (*asterisks*) invading the horizontal branch of the mandible. SUV_{max}, 18. The coronal PET/CT image (*C*) does not show any PNS along the mandibular nerve (V3). However, the corresponding coronal Short-TI Inversion Recovery (STIR) image (*D*) clearly shows thickening of V3 (*arrows*) extending up to the foramen ovale and corresponding to PNS. After IV administration of contrast material, enhancement of the thickened V3 was seen (not shown). Six months after surgery and radiochemotherapy, PNS progressed intracranially.

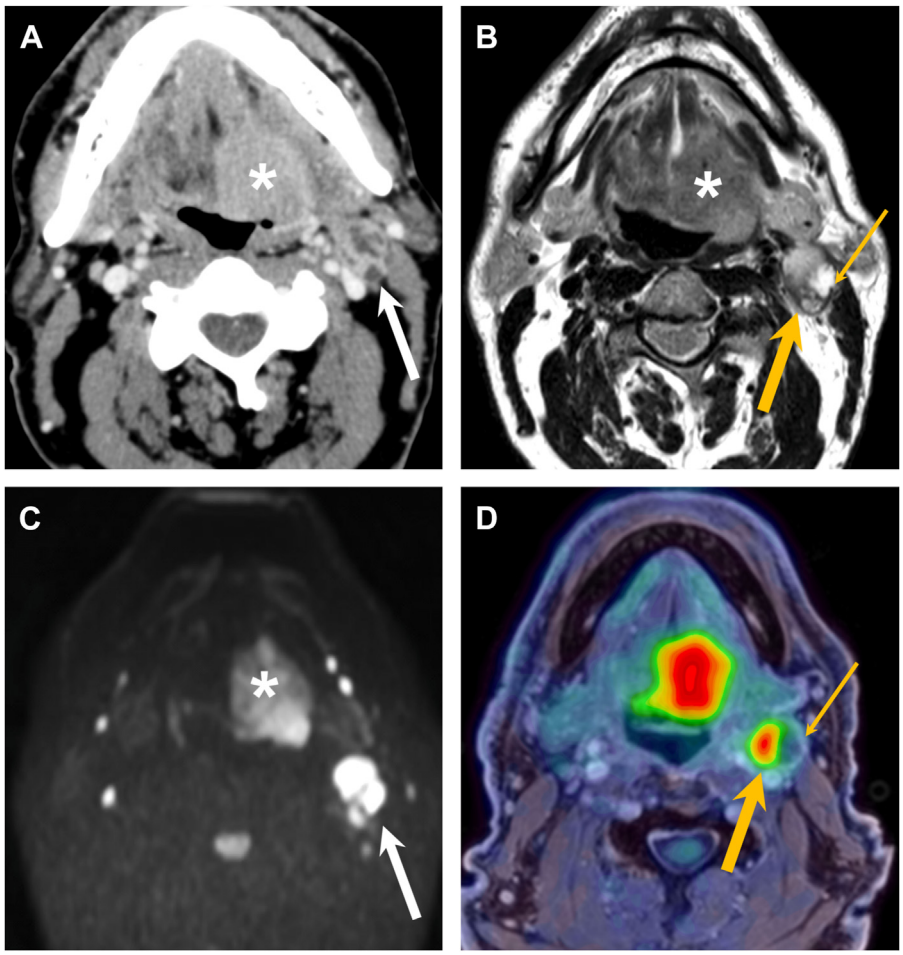

Fig. 7. Characteristic aspect of metastatic lymph nodes on CT and PET/MR imaging. (*A*) Contrast-enhanced CT image obtained in a 58-year-old patient with an HPV positive base of the tongue SCC (*asterisk*). Note an ipsilateral enlarged level II metastatic node (*arrow*) with peripheral rim enhancement and necrotic portions. Corresponding PET/MR imaging obtained at the same level (*B*). T2W image (*C*) b 1000 image from DWI. (*D*) Fused PET and contrast-enhanced Dixon image. The tumor (*asterisks in B and C*) invades the extrinsic tongue muscles and has an intermediate signal intensity on T2, restricted diffusion and increased FDG uptake (SUV_{max} = 15). The solid portions of the level II metastatic node (*thick yellow arrows*) show increased FDG uptake (SUVmax = 14), whereas the necrotic portions (*thin arrows*) show no relevant uptake.

similar sensitivity, specificity, and accuracy in the per-patient analysis (n = 11), per-nodal level analysis (n = 54), and per-node analysis (n = 464), respectively.[40] Inter-reader agreement for PET/MR imaging, PET/CT, and MR imaging was perfect with Cohen kappa values greater than 0.9.[40] Likewise, Platzek and colleagues found no significant differences between PET/MR imaging, PET alone, and MR imaging alone in terms of sensitivity, specificity, and accuracy in their analysis of 391 dissected lymph node levels in 38 patients with HNSCC.[54] In contrast, based on a series of 44 HNSCC patients with clinically N0 necks and neck dissections, Cebeci and colleagues found that PET/MR imaging had a superior sensitivity and negative predictive value (NPV) in comparison to MR imaging alone (sensitivity = 83% vs 50%; NPV = 97% vs 92%, $P < .05$).[55] Likewise, based on the analysis of 865 lymph nodes obtained from neck dissections in 26 patients, Crimi and colleagues found that compared with contrast-enhanced MR imaging alone or PET alone, PET/MR imaging had a superior diagnostic performance.[56] Furthermore, PET/MR imaging with a SUV_{max} cutoff of 5.7 combined with size and/or morphologic MR imaging criteria reached high values for accuracy (98.2%), NPV (98.2%), and positive predictive value (PPV) (95.2%).[56]

Among the studies using the N stage set at the multidisciplinary tumor board (MDTB) as standard

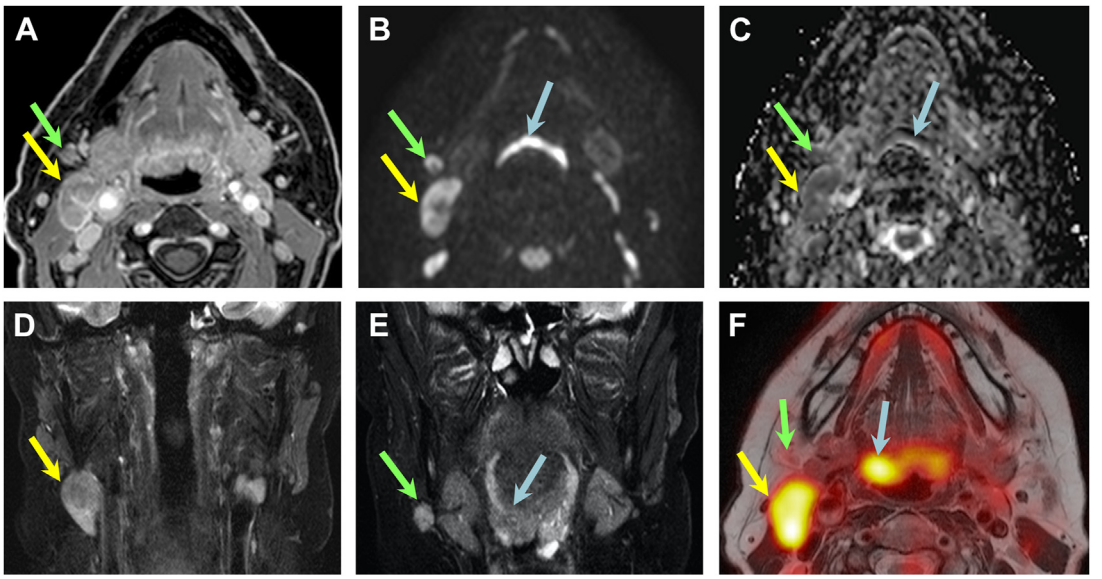

Fig. 8. PET/DWIMR imaging features of metastatic lymph nodes seen in a patient with NCUP. (*A*) Contrast-enhanced Dixon sequence. (*B*) b 1000 image from DWI. (*C*) ADC map from DWI. (*D, E*) Coronal STIR images. (*F*). Fused PET and T2W image. The patient presented with a level II palpable node (*yellow arrows*) which has the characteristic features of a metastatic lymph node (increased size, restricted diffusion with ADC = 0.85 × 10–3 mm^2/s, inhomogeneous enhancement and increased FDG uptake, SUV_{max} = 16). The smaller level Ib node on the right (*green arrows*) is suspicious on MR imaging (rounded shape, irregular contour, low ADC, and inhomogeneous enhancement) but shows no FDG uptake due to its small size. On (*F*), a lesion is seen in the right base of the tongue (*blue arrows*), which was retrospectively also identified on the coronal STIR (*E*). Owing to geometric distortion on DWI, the base of the tongue lesion is not seen. Biopsy-revealed HPV-negative SCC in the base of the tongue. Ultrasonography-guided fine needle aspiration cytology (US FNAC) of level II and level Ib nodes was positive for SCC.

of reference, Flygare and colleagues found that PET/MR imaging was more accurate than PET/CT in 40 patients with oropharyngeal SCC.[43] In the series of Chan and colleagues (113 patients with nasopharyngeal cancer), the standard of reference consisted of the N stage set at the MDTB after having performed ultrasonography-guided fine needle aspiration cytology (US FNAC) or biopsy in cases with discordant imaging findings.[44] The investigators found that the sensitivity of PET/MR imaging (99.5%) was higher than that of PET/CT (91%) or MR imaging alone (94%); PET/MR imaging was particularly useful for distinguishing retropharyngeal nodal metastases from nasopharyngeal tumors.[44]

The above-mentioned studies are based on PET and morphologic MR imaging criteria, and data on the combined PET/DWIMR imaging assessment of lymph nodes in HNSCC are still lacking. In several publications, DWIMR imaging has been shown to have a high diagnostic accuracy for detecting lymph node metastases, including subcentimeter metastatic lymph nodes.[57–60] In a systematic review, Driessen and colleagues reported that the accuracy of DWIMR imaging was 85% to 91% and the NPV was higher than 91% for the assessment of metastatic lymph nodes.[61] Belfiore and colleagues concluded that ADC values can be reliably used to assess metastatic lymph nodes in the neck and that the sensitivity, specificity, and area under the curve (AUC) of a narrower region of interest (ROI) for recognizing metastases were greater compared with the ADC value of the whole node.[62] Several studies on PET, DWI, and MR imaging characteristics of HNSCC lymph nodes have assessed differences between normal and metastatic neck nodes without reporting the diagnostic performance of the respective modalities for N staging.[63,64] From a clinical point of view, it would be very useful to know whether combining morphologic MR imaging criteria with DWI and PET criteria could improve the N staging accuracy in HNSCC.

Detection of Distant Metastases (M staging) and Second Primary Cancers

Distant tumor spread includes hematogenous spread to distant organs and lymphatic spread to distant lymph nodes. Up to 28% of patients with primary and recurrent HNSCC have metastases or second primary cancers at the time of

diagnosis.[24,65,66] These second primary cancers originate within the HN region or in distant sites (eg, lung, esophagus, or colon). Most of the HNSCC metastases are found in the lungs or mediastinum, whereas bone and liver metastases are uncommon. In a prospective study evaluating distant metastases and second primary cancers in 82 HNSCC patients undergoing PET/MR imaging and PET/CT, Katirtzidou and colleagues reported that patients imaged for follow-up/suspected HNSCC recurrence had a higher incidence of distant malignant lesions compared with patients with primary tumors or NCUP; the standard of reference was histology and follow-up greater than 2 years or until death.[24]

In the past, HNSCC patients with distant metastases were treated only palliatively and screening for distant metastases aimed to avoid aggressive locoregional treatment. However, in recent years, as oligometastases are treated by metastasectomy or stereotactic radiotherapy, the therapeutic paradigm in HNSCC patients has changed.[67] In addition, there is a growing body of evidence supporting the implementation of whole-body MR imaging or FDG PET/MR imaging for the detection of distant metastases.[67–69]

In a prospective study enrolling 198 patients with primary oropharyngeal and hypopharyngeal SCC, Yeh and colleagues found a similar PET/MR imaging and PET/CT sensitivity for the detection of second primary cancers and metastases to neck nodes and distant sites (73.5% vs 69.9%, $P = .08$) and there were no significant differences in terms of diagnostic capability between MR imaging and PET/CT (AUC = 0.905 vs 0.917, $P = .469$) and between PET/MR imaging and PET/CT (AUC = 0.930 vs 0.917, $P = .062$), respectively; the standard of reference was biopsy and follow-up greater than 1 year or until death.[66]

In contrast to the study of Yeh and colleagues, Katirtzidou and colleagues specifically focused on malignant lesions outside the HN area. In a prospective study including 103 examinations in 82 HNSCC patients with 183 distant lesions, the investigators reported that PET/MR imaging had a similar and high diagnostic performance as PET/CT for the detection of distant malignant lesions (metastases and second primary cancers), regardless of the type of analysis conducted (AUC per patient = 0.947 vs 0.975; AUC per examination = 0.965 vs 0.968; AUC per lesion = 0.957 vs 0.944, $P > .05$) (**Figs. 9–11**). Depending on the analysis type (per patient, per examination, per lesion), the sensitivity, specificity, and accuracy varied between 94%–96%, 85%–90%, and 89%–91% for PET/MR imaging and 90%–96%, 86%–93%, and 88%–93% for PET/CT, respectively; all pairwise comparisons yielded P values > 0.05.[24] Furthermore, the findings in this study suggested that due to the high occurrence of distant metastases and second primary cancers during follow-up, imaging with FDG PET/CT or FDG PET/MR imaging outside the HN area should be considered more frequently. As FDG PET/MR imaging has shown excellent results in detecting local recurrence after radio(chemo)therapy,[13] the investigators suggested that whole-body PET/MR imaging could reliably complement locoregional PET/MR imaging assessment.[24]

Based on a meta-analysis including 14 studies (1042 patients), Zhang and colleagues reported a higher sensitivity of FDG PET/MR imaging compared with PET/CT (0.87 vs 0.81), a higher AUC value (0.98 vs 0.95), and similar specificity (0.97 vs 0.97) for detecting distant metastases.[70] This meta-analysis included, however, different cancer types, for example, breast and lung cancer, which are known to be more commonly associated with bone metastases than HNSCC.[71] The investigators also noted that FDG PET/MR imaging and PET/CT had different diagnostic performances in different tumors types, for example, the accuracy of PET/MR imaging was higher in patients with breast cancer, whereas the accuracy of PET/CT was higher in patients with lung cancer.[70]

As most HNSCC patients develop distant malignant lesions in the lungs (and rarely in the bones), it is important to be aware of the diagnostic PET/MR imaging performance for lung nodules. Several investigators have suggested that PET/MR imaging can reliably detect and characterize FDG-avid pulmonary lesions.[68,69,72] In a study involving patients with different types of primary cancers, Chandarana and colleagues showed that PET/MR imaging had a high sensitivity for the detection of FDG-avid nodules (96%) and nodules greater than 0.5 cm in diameter (89%), with a low sensitivity for small non-FDG-avid nodules.[68] Likewise, Lee and colleagues reported a high detection rate for FDG-avid pulmonary nodules (sensitivity = 98%) with PET/MR imaging in a series of 51 patients with different cancer types, whereas the sensitivity for non-FDG-avid small nodules was only 35%.[69] The FDG-avidity of tumors is influenced by their histology, which impacts the diagnostic performance of FDG PET. Therefore, it is essential for studies to consider this aspect. As metastases and distant second primary cancers in HNSCC patients are mostly FDG-avid, the detection rate in HNSCC is high and similar with PET/MR imaging and PET/CT. Furthermore, the study of Katirtzidou and colleagues found that FDG-negative lung nodules $\leq$8 mm in HNSCC patients were predominantly benign.[24] It is worthwhile mentioning that

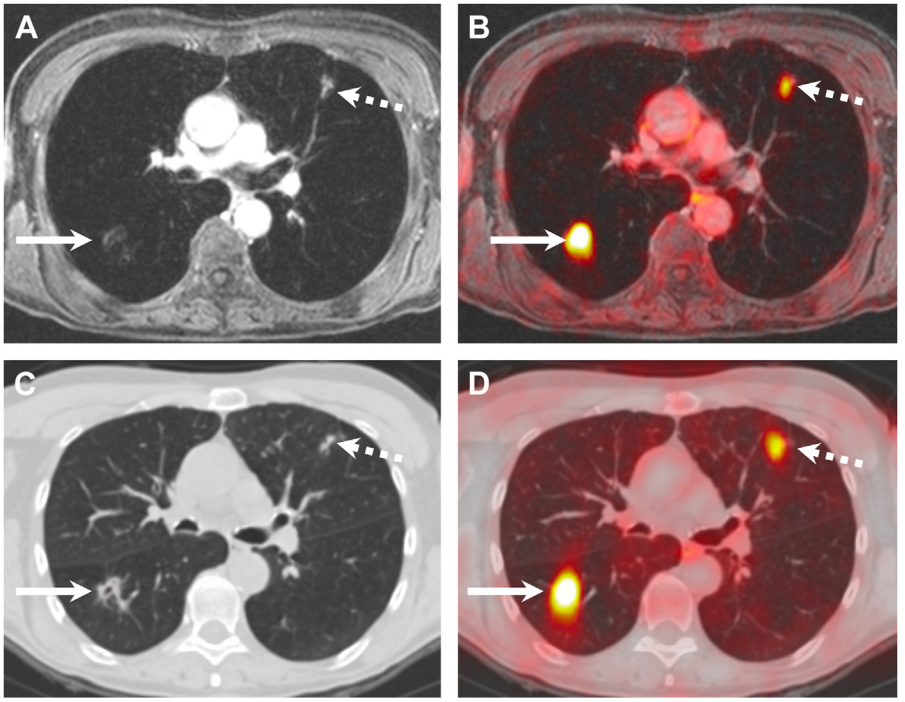

Fig. 9. Lung metastases correctly diagnosed on PET/MR imaging (*A, B*) and PET/CT (*C, D*) in a 60-year old woman with nodal recurrence after radiochemotherapy for oropharyngeal HPV-negative SCC. The right upper lobe metastasis (*arrows*) shows a combination of high focal FDG uptake (SUVmax on PET/MR imaging = 7.7 and SUVmax on PET/CT = 9.3) and an excavated aspect on the contrast-enhanced fat-saturated MR image and on the corresponding CT image. The left upper lobe metastasis (*dashed arrows*) displays minor focal FDG uptake (SUVmax on PET/MR imaging = 1.7 and SUVmax on PET/CT = 2.1) and clustered nodules on the corresponding morphologic MR imaging/CT images. Both lesions were rated with a score of 5 (highly suspicious) on PET/MR imaging and PET/CT. (*Reproduced from* Katirtzidou et al.[24])

false positive evaluations due to high FDG uptake can also occur (especially in the mediastinum) and depending on the clinical situation, biopsy is mandatory (**Fig. 12**).

In conclusion, the current literature suggests that both PET/MR imaging and PET/CT have a high and comparable diagnostic performance for the detection of distant metastases and distant second primary cancers in HNSCC patients.

NECK CARCINOMA OF UNKNOWN PRIMARY

Historically, 1%–9% of HNSCC were considered as NCUP.[73] However, during the past decades, the incidence of NCUP has increased due to the increasing incidence of HPV-positive oropharyngeal SCC, which often presents clinically as NCUP. The 8th edition of the TNM staging manual classifies HPV-positive NCUP as HPV-positive oropharyngeal SCC.[74]

The guidelines for the workup of NCUP include US FNAC or US-guided biopsy of the enlarged neck node (with p16 immunohistochemistry and direct HPV testing), PET/CT, MR imaging, endoscopic biopsy under general anesthesia, tonsillectomy, and more recently narrow band imaging and tongue base mucosectomy.[73,75] Narrow band imaging uses blue and green light with different wavelengths to optimize visualization of mucosal microvascular changes as seen in dysplasia and malignancy.

In most studies, the reported rates of NCUP identification with FDG PET/CT remain below 55%.[73,76–78] In contrast, only one study including 30 NCUP patients reported a sensitivity of 94%.[10] Most investigators agree that FDG PET/CT has a relatively high number of false positives (up to 40%) due to the physiologic uptake of oropharyngeal lymphoid tissue.[10,73,78] Nevertheless, FDG PET/CT enables the detection of additional metastatic lymph nodes and distant metastases.[78] Recently, Noji and colleagues reported that the sensitivity and specificity of qualitative and quantitative analysis with DWIMR imaging and FDG PET/CT were similar; however, adding DWIMR imaging did not improve the accuracy of FDG PET/CT.[10] An important limitation of most published studies is the fact that most series

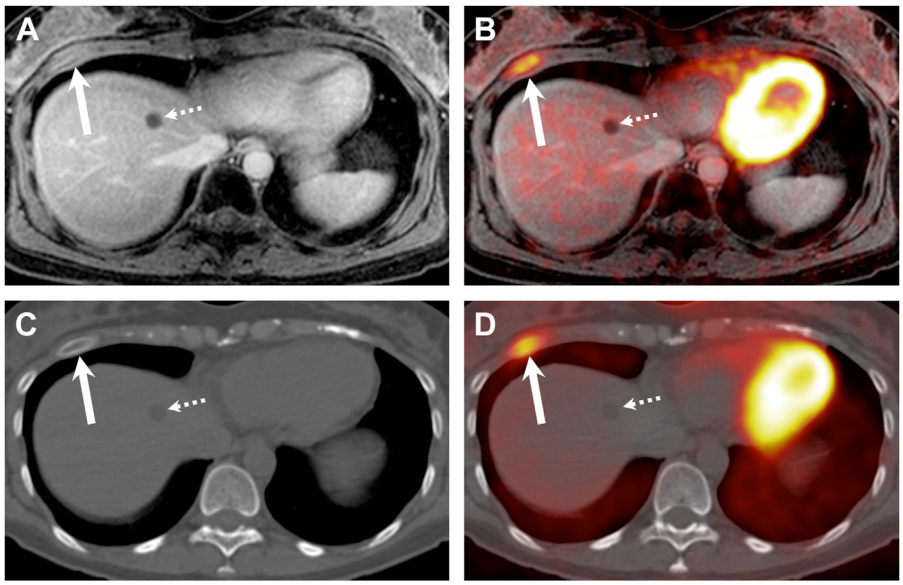

Fig. 10. Rib metastasis detected on both PET/MRI (*A, B*) and PET/CT (*C, D*) in a 42-year old female without locoregional recurrence after radiochemotherapy for an SCC of the paranasal sinuses. The rib lesion (arrows on all images) shows a combination of high focal FDG uptake (SUVmax on PET/MR imaging = 6.3 and SUVmax on PET/CT = 4.7) and an expansile aspect on MR imaging/CT. Note lesion enhancement on the contrast enhanced fat saturated MR image. The lesion was rated with a score of 5 (highly suspicious) on PET/MR imaging and with a score of 4 (moderately suspicious) on PET/CT. Dashed arrows point at a liver cyst. (*Reproduced from* Katirtzidou et al.[24])

included only a small number of patients. In the only study published so fat directly comparing the diagnostic performance of FDG PET/CT with PET/MR imaging (without DWI), Ruhlmann and colleagues found a similar diagnostic ability for the detection of primary cancer and metastases in 20 patients with NCUP.[78]

Based on the current literature, no evidence-based conclusion can be drawn about the role of PET/MR imaging ± DWI in the workup of NCUP and further studies are warranted.

TUMOR SEGMENTATION

Curative treatment options for patients with HNSCC include surgery and radio(chemo)therapy. Regardless of the chosen treatment, precise and accurate delineation of tumor margins and, therefore, tumor volume are fundamental for effectively managing patients with HNSCC. In surgical procedures, a delicate trade-off must be achieved between a limited tumor resection with the risk of positive or close margins (associated with poorer prognosis) and a wide resection (leading to unsatisfactory functional and cosmetic outcomes).

In terms of tumor volume, radiation oncologists distinguish between gross tumor volume (GTV, which is the delineated radiologically measurable tumor), clinical target volume (CTV, which adds a margin to the GTV to cover areas of potential microscopic disease), and planning target volume (PTV, defined as the CTV surrounded by adequate margins to account for organ and patient motion or variation in patient position). Although the adoption of intensity-modulated radiation therapy protocols has reduced irradiation volumes on the one hand (thus avoiding irradiation of organs at risk), it has also increased the importance of precise GTV delineation on the other hand.[79–81] Precise delineation of GTVs has not only a direct impact on patient outcome but it can also jeopardize the robustness of quantitative metrics, including radiomics features.[82]

Although contrast-enhanced CT is a standard imaging technique for radiation therapy planning in HNSCC, it falls short in precisely delineating GTVs of primary tumors and lymph node metastases. Incorporating PET data into radiation therapy planning offers several advantages over using CT alone.[79] By using FDG PET, the risk of inaccurately targeting radiation delivery to the intended volumes is reduced.[83,84] In addition, the use of other radiotracers, such as 18F-fluoromisonidazole, a biomarker for hypoxia, can identify tissues that require intensified treatment approaches.[85] Beyond PET biomarkers, functional MR imaging biomarkers provide the ability to characterize cellularity, vascularity, and permeability of tumors,

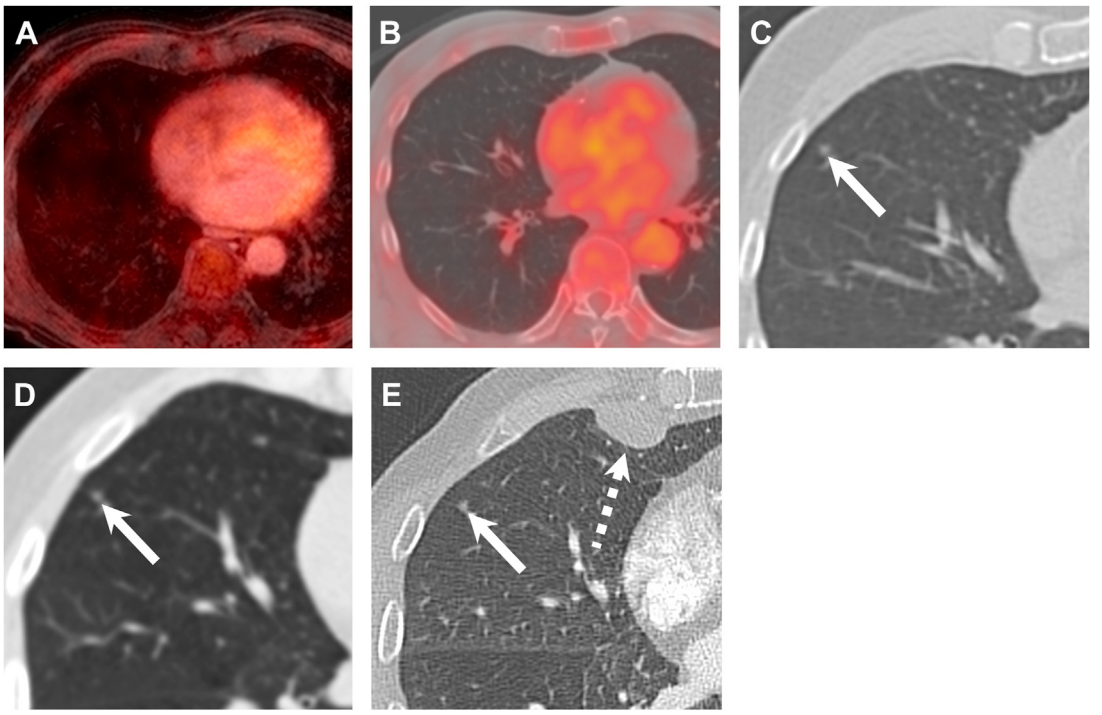

Fig. 11. False-negative PET/MR imaging (*A*) and PET/CT (*B*) in an 89-year-old man with primary SCC of the oral cavity. Both PET/MR imaging and PET/CT were rated as negative for distant metastases or second primary cancers (diagnostic score = 1). PET/MR imaging (*A*) shows no lesion. PET/CT (*B*) and detail of the corresponding CT component of the PET/CT (*C*) show a non-FDG avid 5 mm solid lung nodule (*arrow* in *C*), which was considered as benign according to diagnostic criteria (no FDG uptake and $\leq$8 mm in size). The lesion was rated with a score of 1 on PET/MR imaging and PET/CT. Follow-up CT obtained 2 months later (*D*) showed no change in size and shape of the 5 mm nodule (*arrow*). CT obtained 7 months later (*E*) revealed no change in the 5 mm nodule (*arrow*), however, a pleural metastasis (*dashed arrow*) that was confirmed histologically. As the pleural metastasis occurred within the 2-year follow-up, both PET/CT and PET/MR imaging were considered as false negative. In this study, criteria for progression were an increase in lesion size during follow-up or the appearance of new lesions within 2 years. A greater than 2-year follow-up period was chosen as distant metastases/second primary cancers may be subclinical at initial imaging, and depending on tumor kinetics and patient immune status, they may show only minimal changes over time. (*Reproduced from* Katirtzidou et al.[24])

thus leading to a more accurate representation of the biological tumor volume.[30,86]

Against this background, the focus of attention has recently shifted toward multimodality PET/MR imaging or PET/CT/MR imaging-guided estimation of GTV.[79,87] Nevertheless, published data on this topic are very scarce. Moreover, most studies are based on small series without histopathologic correlation and GTVs defined on planning CT or on morphologic MR images were used as standard of reference (ground truth). In a prospective study including 11 patients with HNSCC, Wang and colleagues compared primary and nodal GTVs delineated on CT (ground truth) with the corresponding GTVs delineated on PET/MR imaging; the investigators found that PET/MR imaging- and CT-derived GTVs were similar. However, the Dice similarity coefficient (DSC), a metric evaluating the spatial overlap between two measured volumes, was only 0.63 to 0.69 (DSC range = 0–1, with 1 indicating perfect match), and the modified Hausdorff distance (ie, the orthogonal distance difference between CT and PET/MR imaging segmentation) was 1.6 to 2.3 mm.[88] Samolyk-Kogaczewska and colleagues evaluated the usefulness and accuracy of PET/MR imaging GTV delineation by radiation oncologists in 10 patients with SCC of the tongue.[89] The GTVs for primary tumors and lymph nodes defined on CT (ground truth) were compared with the GTVs delineated on PET/MR imaging. The investigators found that in 7/10 patients, the volumes were smaller on PET/MR imaging than on CT. The investigators also analyzed which SUV_{max} threshold best matched the ground truth, and they reported best results for 30% SUV_{max} for tumors and 30%–40% SUV_{max} for lymph nodes, respectively.[89] Bird and colleagues found significant

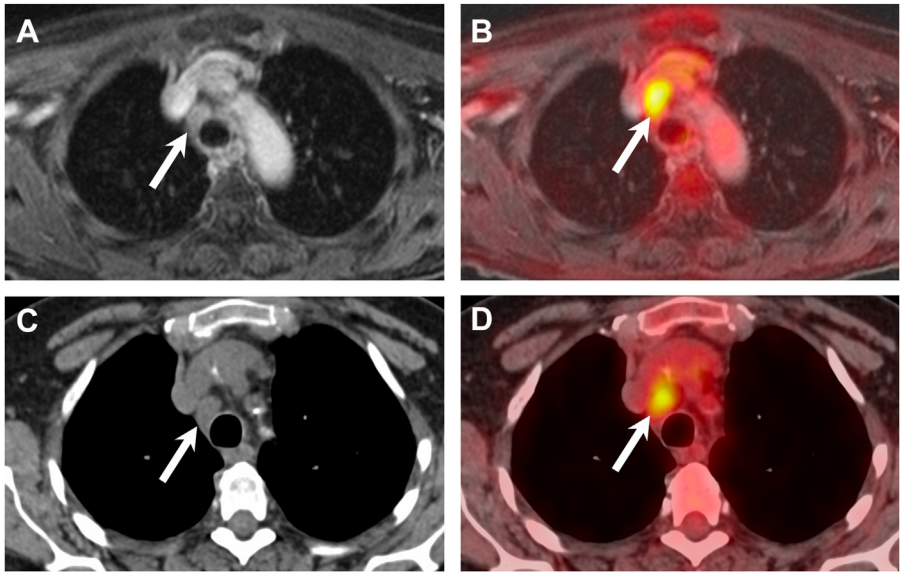

Fig. 12. False-positive PET/MR imaging (*A,B*) and PET/CT (*C,D*) in a 63-year old woman imaged for follow-up of an SCC of the larynx (T3N1) treated with radiochemotherapy. Both PET/MR imaging and PET/CT were rated as positive for distant mediastinal lymph node metastases. An enlarged mediastinal lymph node (*arrows*) shows a combination of high focal FDG uptake (SUVmax on PET/MR imaging = 7.5 and SUVmax on PET/CT = 6.7) and slightly heterogeneous contrast enhancement on the contrast-enhanced fat-saturated MR image. On the corresponding CT image, due to the absence of contrast enhancement, only lymph node enlargement was present (13 × 15 × 17 mm). The lymph node was rated with a score of 5 (highly suspicious) on PET/MR imaging and a score of 4 (moderately suspicious) on PET/CT. However, mediastinoscopy with biopsy-revealed sarcoidosis. (*Reproduced from* Katirtzidou et al.[24])

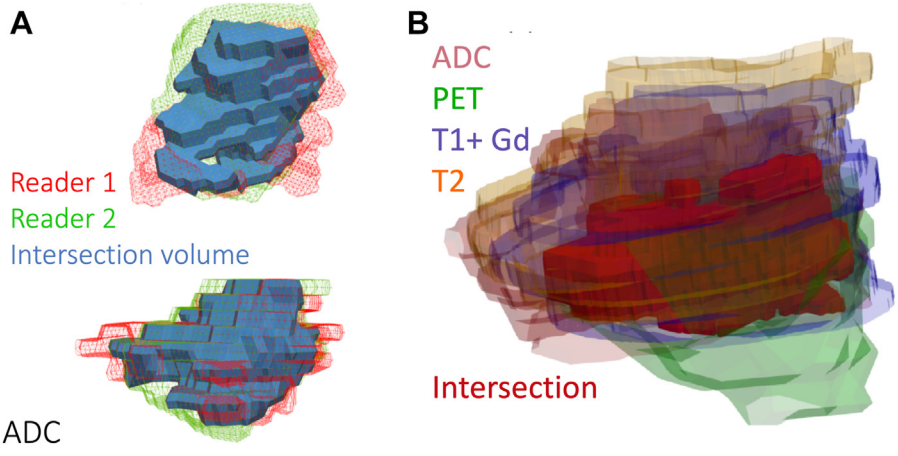

Fig. 13. The complexity of multiparametric segmentation with 3D rendering of the segmented GTVs. (*A*) Segmentation of an oropharyngeal SCC based on the ADC map. Two different readers (a radiation oncologist and a specialized head and neck radiologist) segmented the tumor. The intersection volume is indicated in blue. (*B*) Segmentation of the same oropharyngeal SCC by one reader based on a multiparametric PET/MR imaging acquisition (ADC, PET, contrast-enhanced T1 and T2 images). The intersection volume is rendered in dark red. Note that there is neither a perfect overlap between the GTVs contoured on the different modalities nor between the two readers.

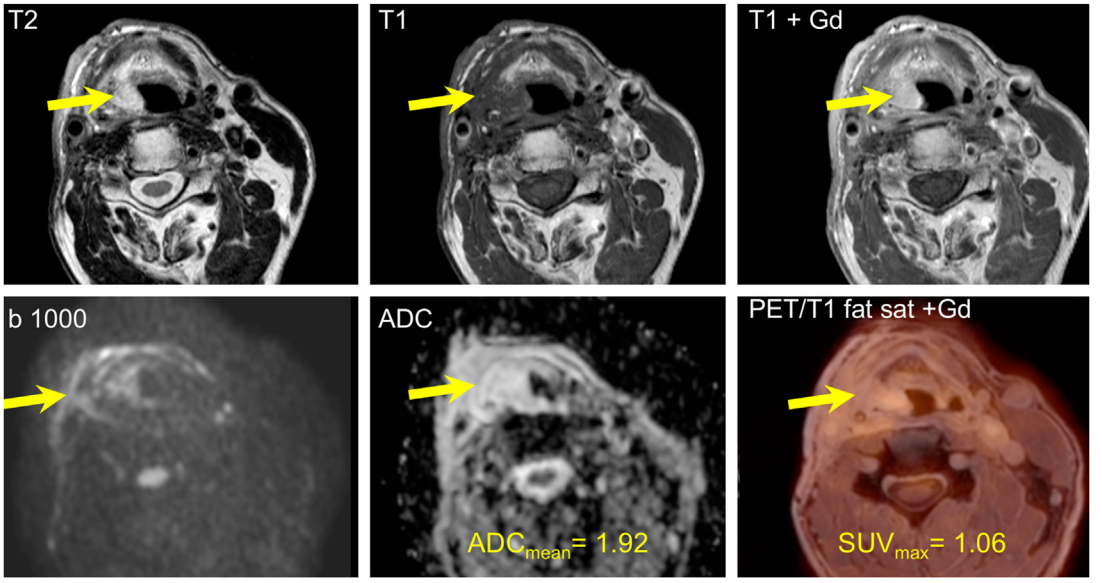

Fig. 14. Posttreatment inflammatory edema in a patient with radiochemotherapy and neck dissection for an SCC of the oral cavity. Note a poorly delineated area with high signal intensity on T2, major contrast enhancement, no restriction of diffusion and no relevant FDG uptake (*yellow arrows*).

differences in mean GTVs between CT, MR imaging, PET, and combinations thereof in 11 patients with locally advanced oropharyngeal SCC with no single imaging technique encompassing all potential GTV regions.[90] The investigators also found that the use of MR imaging reduced interobserver variability.

In the only study published so far using histopathology of the resected specimen as ground truth and GTV contoured on a modern PET/MR imaging hybrid system, Terzidis and colleagues compared the pathologic GTVs obtained from 13 surgical HNSCC specimens (GTV$_{patho}$) with the corresponding CTVs delineated on PET/MR imaging in

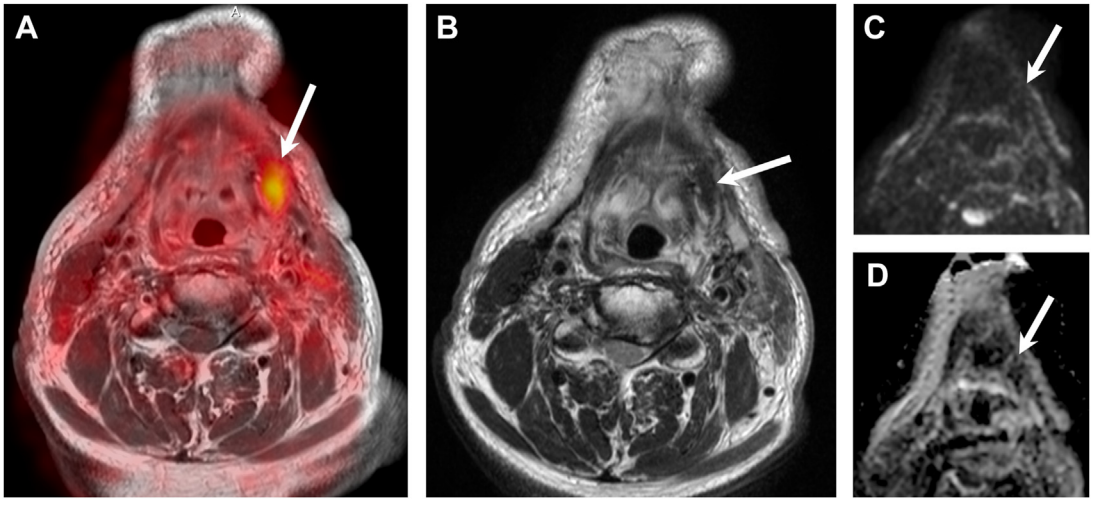

Fig. 15. Posttreatment scar in a patient with radiotherapy, partial pelviglossectomy and left neck dissection for an SCC of the oral cavity. Images obtained from a PET/DWIMR imaging examination. (*A*) Fused PET with contrast-enhanced T1W image (*arrow*). (*B*) Corresponding T2W image. (*C*) b 1000 image. (*D*) ADC map. Note an area of focal uptake on the fused PET and contrast-enhanced T1W image. SUV$_{max}$ = 9. The T2W image shows an area with very low signal intensity (*arrow*) corresponding to mature scar tissue. On DWI, a T2 black-out effect (*arrows*) is seen resulting in a low ADC value (ADC = 0.93 × 10–3 mm^2/s).

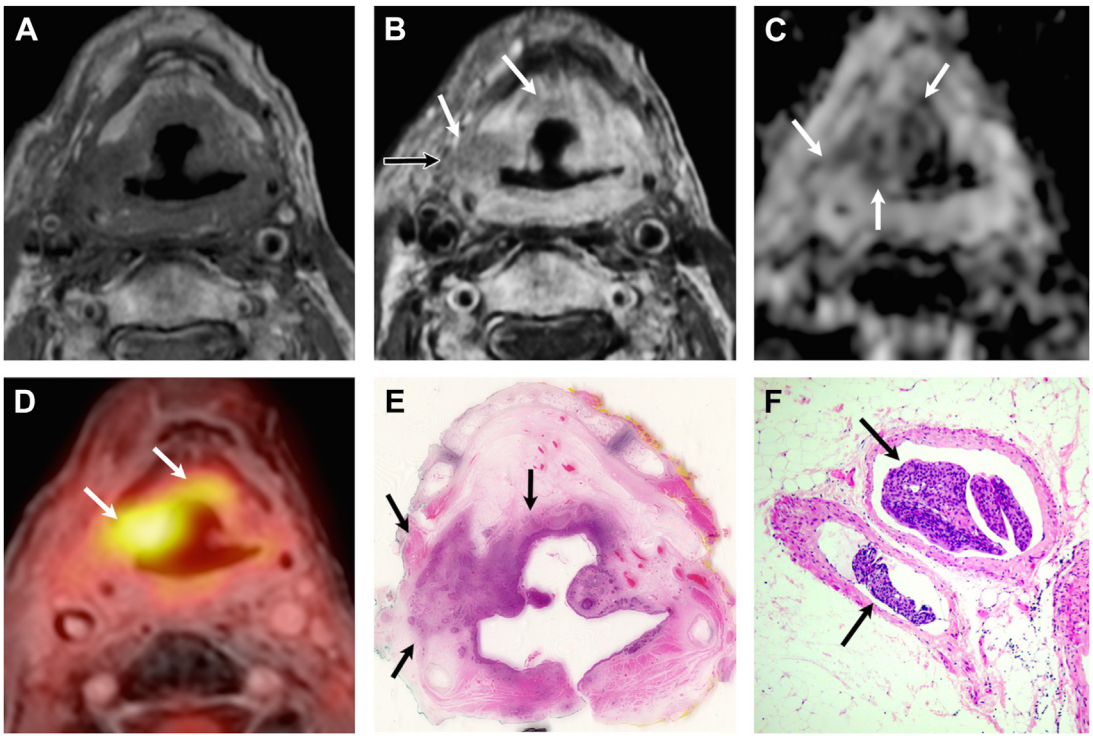

Fig. 16. True positive evaluation with combined PET/DWIMR imaging (positive concordant findings on MR imaging, DWI, and PET). A 69-year-old man with pain 4 years after radiochemotherapy for SCC of the hypopharynx. Unenhanced T1 (*A*): poorly defined hypointensity in both aryepiglottic folds, pre-epiglottic space, and retropharyngeal space. Contrast-enhanced T1 (*B*): infiltrative, moderately enhancing lesion (*white arrows*) in the right paraglottic and pre-epiglottic space with invasion into the soft tissues of the neck (*black arrow*) suggesting recurrence. Note strongly enhancing retropharyngeal space and left aryepiglottic fold due to inflammatory edema. (*C*) ADC map: restricted diffusion on the right (*arrows*, ADCmean = 0.997 $\times$ 10^{-3} mm^2/s) consistent with recurrence. High signal in the left paraglottic space and retropharyngeal space (ADCmean = 1.815 $\times$ 10^{-3} mm^2/s) due to inflammatory edema. (*D*) PET/MR imaging (PET fused with gadolinium-enhanced Dixon) consistent with recurrence (*arrows*, SUVmean = 4.417; SUVmax = 5.518). (*E*) Corresponding whole-organ axial histologic section (hematoxylin-eosin, HE) confirms recurrence on the right (*arrows*) and inflammatory edema on the left and in the retropharyngeal space. (*F*) Section from right specimen periphery (HE, original magnification 100 $\times$) depicts venous tumor thrombi (*arrows*). T stage on PET/DWIMR imaging was T4a. Pathologic stage was pT4a. (*Reproduced from* Becker et al 2018.[6])

combination with clinical information ($GTV_{oncologic}$).[80] The mean tumor volume defined by PET/MR imaging and clinical information ($GTV_{oncologic}$) was larger than the tumor volume defined at histopathology. The mean mismatch between the GTV_{patho} and the $GTV_{oncologic}$ (ie, the percentage of GTV_{patho} not encompassed in the $GTV_{oncologic}$) was 27.9% and in 12/13 patients GTV_{patho} was not fully encompassed in the $GTV_{oncologic}$. Nevertheless, an isotropic 5 mm expansion to $GTV_{oncologic}$ was sufficient to cover the GTV_{patho}.[80] The investigators concluded that despite modern PET/MR imaging technology, a mismatch between imaging and GTV_{patho} was observed in all patients.[80] They also pointed out that reducing margins by even 1 mm may increase the proportion of tumor outside the radiotherapy target volume, which could explain recurrences at the periphery of GTVs delineated for radiotherapy treatment planning.[80]

In routine clinical work, GTVs and CTVs are contoured manually by radiation oncologists. However, this time-consuming task suffers from subjectivity, interobserver variability, and other factors affecting human expertise. For example, recent publications have shown that the review of oncologist-delineated radiotherapy target volumes by specialized HN radiologists changes 52%–55% of volumes delineated on CT or MR imaging.[91,92] Moreover, Adjogatse and colleagues reported that MR imaging-based peer review by specialized HN radiologists altered 76% of GTVs and 41.5% of gross nodal volumes with 55% of GTV and 67% of gross nodal volume alterations classified as

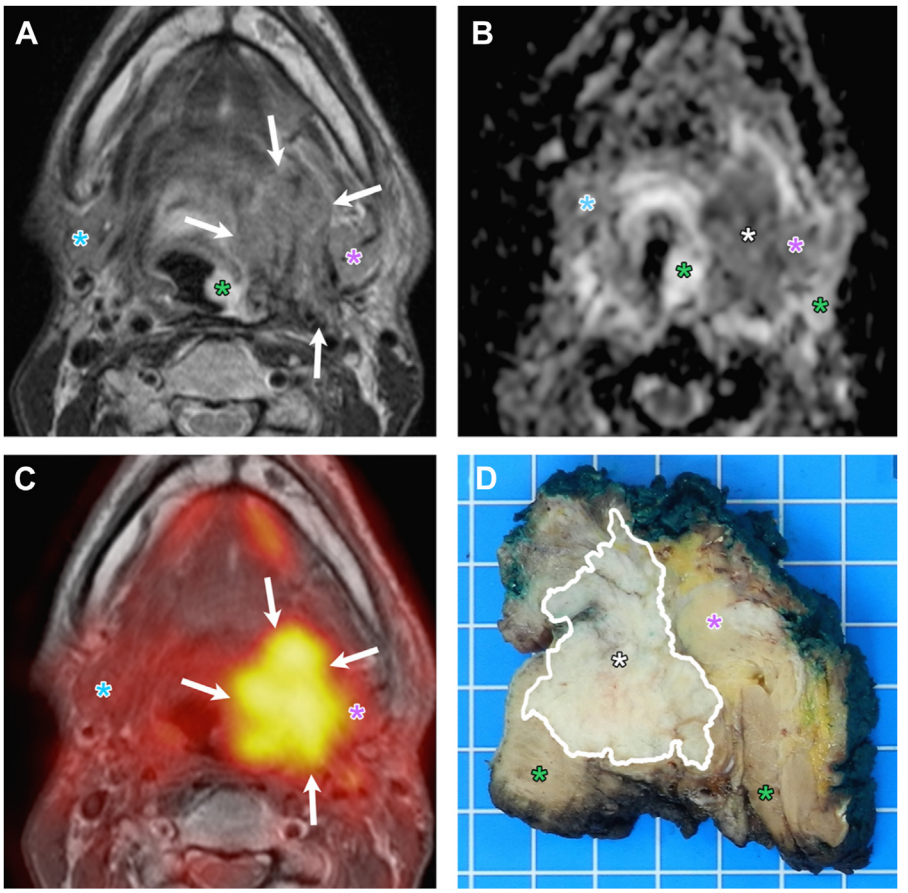

Fig. 17. True positive evaluation with combined PET/DWIMR imaging (positive concordant findings on MR imaging, DWI, and PET). A 48-year-old man with reflex otalgia 1 year after radiochemotherapy for SCC of the base of the tongue. Endoscopy: edema and intact mucosa. T2 (*A*) infiltrative tumor recurrence with intermediate signal (*arrows*) in the left tongue base, extrinsic tongue muscles, vallecula, and parapharyngeal space. Suspected invasion of the left submandibular gland (*pink asterisk*). Submucosal edema with very high T2 signal (*green asterisk*). Normal right submandibular gland (*blue asterisk*). ADC map (*B*) restricted diffusion suggesting recurrence (*white asterisk*, ADCmean = 1.127×10^{-3} mm^2/s). High ADC signal surrounding the tumor (*green asterisks*, ADCmean = $1.789–1.965 \times 10^{-3}$ mm^2/s) due to edema. Left and right submandibular glands (*pink and blue asterisks*). (*C*) PET/MR imaging (PET fused with T1) suggests recurrence (increased FDG uptake, *arrows*, SUVmean = 7.688; SUVmax = 12.11). Left and right submandibular glands (*pink and blue asterisks*). (*D*) Whole-organ axial section from surgical specimen (same orientation) confirms recurrence (*white asterisk*) invading the above-described structures. Submandibular gland (*pink asterisk*). Tumor margins contoured by pathologist (*white line*). Green asterisks: *inflammatory edema*. T-stage on PET/DWIMR imaging was T4a. Pathologic stage was pT4a. (*Reproduced from* Becker et al 2018.[6])

"major." Undercontouring of soft tissue involvement and unidentified lymph nodes were main reasons for change.[81] Therefore, some institutions have already introduced a formal MR imaging-based radiology review of oncologist-delineated target volumes into the radiotherapy workflow for patients with HNSCC.[81]

As we can see from these different studies, manual tumor segmentation has inherent drawbacks related not only to factors affecting human expertise but also because of lacking availability of specialized manpower for peer review of contoured GTVs. Therefore, advanced computational approaches such as DL models hold promise to standardize and fully automatize tumor segmentation and to improve consistency and accuracy in target definition for radiotherapy.[93] As the development of DL models requires very large data sets, which usually cannot be obtained in a single center and as data acquired in a single center may be too homogeneous, therefore impeding generalizability, current DL approaches for HNSCC segmentation are based on centralized or on federated frameworks, which incorporate data from many different

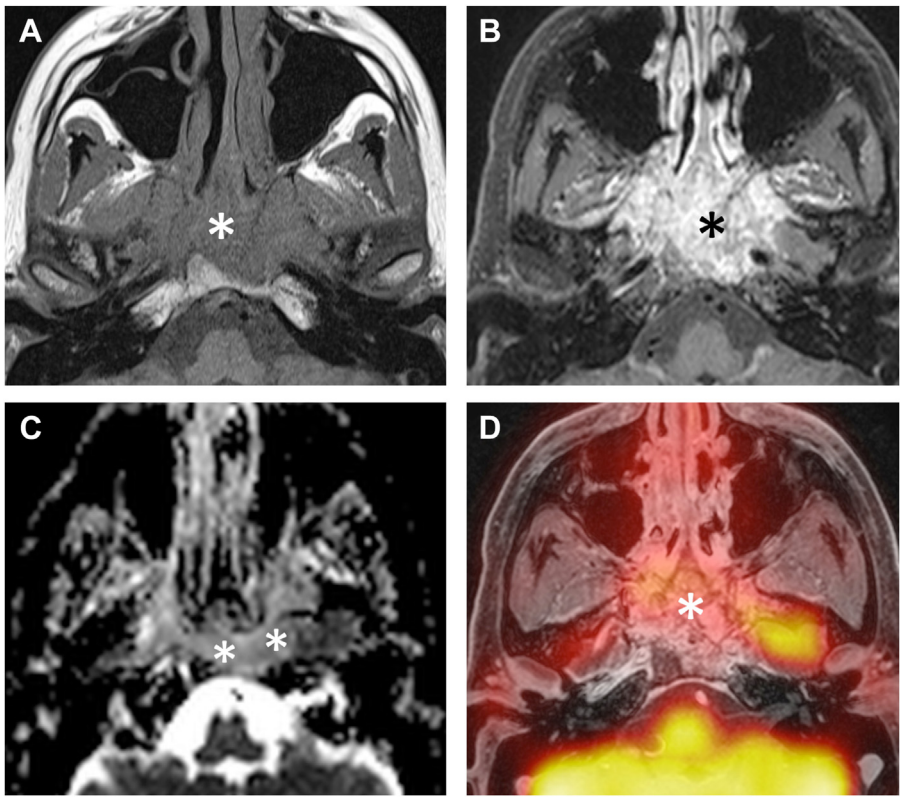

Fig. 18. PET/MR imaging obtained 6 months after proton therapy and chemotherapy for undifferentiated sinonasal carcinoma. Recurrence in the nasopharynx was suspected clinically. (*A*) Axial T1W image shows a large hypointense nasopharyngeal mass (*asterisk*). (*B*) Corresponding fat-saturated gadolinium-enhanced T1W shows that the nasopharyngeal mass (*asterisk*) invades the clivus and central skull base, suggesting recurrence versus radiation-induced inflammation. (*C*) ADC map reveals restricted diffusivity (ADC_{mean}, 0.98 × 10–3 mm^2/s) suggesting recurrence (*asterisks*). (*D*) Corresponding fused PET and gadolinium-enhanced fat-saturated T1 reveal absent FDG uptake (*asterisk*) suggesting inflammation. Surgical biopsy and follow-up greater than 3 years revealed inflammatory tissue. (Images *B, C,* and *D reproduced from* Becker et al 2014.[1])

centers.[82,94–96] In the centralized framework, the centers send their data to a central server with significant computational power, whereas in the federated framework, the users train DL models locally and then send the data to a central server; the central server then aggregates the local updates into a global network. The decentralized federated framework has the advantage of addressing privacy concerns as well as ethical and legal issues.[97] Based on PET images only, Shiri and colleagues have shown that the performance of DL approaches for the segmentation of HNSCC is nearly identical for the centralized and federated approach, both approaches having a DSC of 0.84 and a negligible percent relative error for SUV_{max} compared with manual specialist tumor segmentation. In addition, PET/CT information fusion has been shown to outperform segmentation tasks based on PET only and CT only images, conventional image level, and DL fusions achieving competitive results.[96] Future challenges for DL-based segmentation of HNSCC include segmentation tasks based on multimodality PET/DWI/MR imaging information (Fig. 13).

EVALUATION OF TREATMENT RESPONSE AND DETECTION OF RECURRENT DISEASE

Recurrence in HNSCC is relatively common and depends on patient age, tumor subsite and stage, histologic differentiation, and treatment type. Most recurrences occur at the site of the primary tumor within 2 to 3 years after treatment. Irrespective of tumor type, early detection of recurrent disease is crucial. However, endoscopic and clinical follow-up may miss recurrent disease, especially after radiotherapy due to radiation-induced changes (edema, fibrosis, soft tissue, cartilage, or bone necrosis).

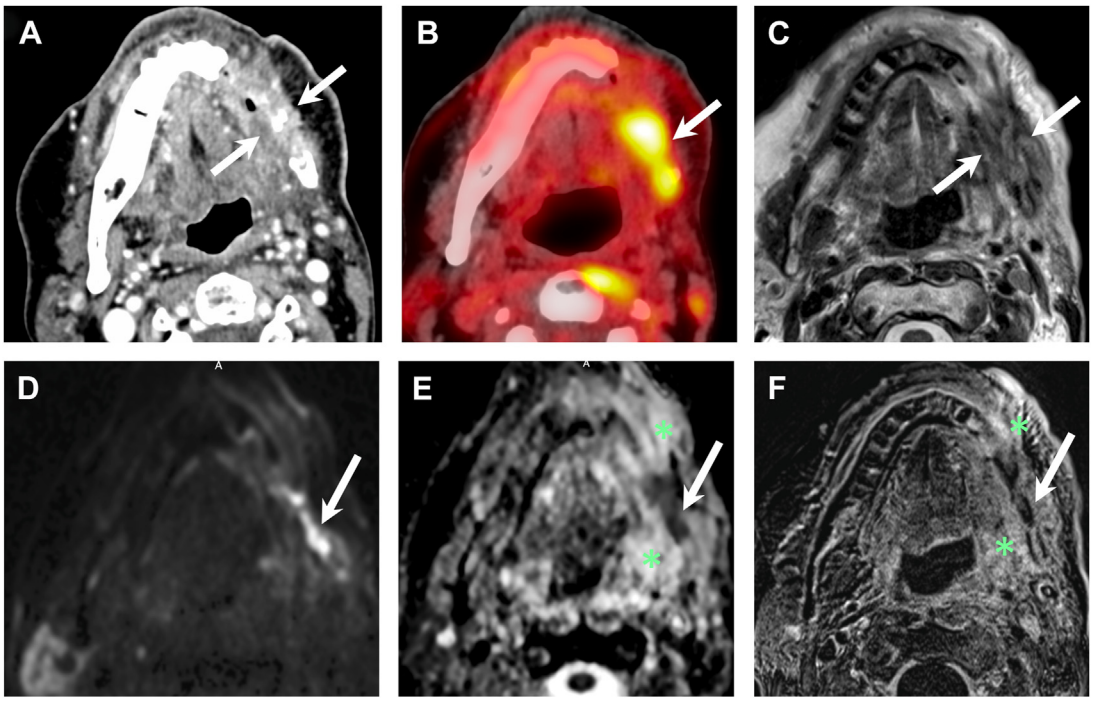

Fig. 19. (*A*) Contrast-enhanced PET/CT and corresponding DWIMR imaging obtained in a 70-year-old patient with radiotherapy for SCC of the oropharynx 3 years previously. (*A*) Contrast-enhanced CT. (*B*) Fused PET and unenhanced CT image. (*C*) T2W image. (*D*) b 1000. (*E*) ADC map. (*F*) Subtraction image (T1W image was subtracted from the contrast-enhanced T1W image). On CT, an enhancing lesion (*arrows*) surrounding the fragmented horizontal branch of mandible is seen on the left. Strong FDG uptake (SUV_{max}, 16). On PET/CT, it is difficult to distinguish between osteoradionecrosis and recurrent SCC or a combination of both entities. There is an intermediate signal intensity on T2 within the mandible and in the soft tissues surrounding the mandible (*arrows*). On DWI, there is restriction of diffusivity (*arrows*) within the mandible but the area with restricted diffusivity does not show enhancement on F (*arrow*). This aspect strongly suggests osteoradionecrosis of the mandible. The soft tissues surrounding the mandible have an increased diffusivity and strong enhancement (*green asterisks on E and F*). They correspond to inflammation. The patient underwent hyperbaric oxygen therapy and 1 year later, there is still no evidence of recurrent SCC.

Studies evaluating the diagnostic performance of PET and PET/CT for the follow-up of HNSCC found that the sensitivity and NPV of PET and PET/CT for detecting residual/recurrent HNSCC at the primary site were very high, however—due to posttreatment inflammatory changes—the specificity and PPV were limited—especially on the baseline scan at 12 weeks after radiotherapy.[98–100] Several investigators have reported a high sensitivity and specificity with DWIMR imaging to detect posttreatment HNSCC recurrence; however, the PPV and NPV varied significantly among the different studies.[101–103] These discrepant DWIMR imaging results can be explained by the fact that different MR imaging criteria and different DWI protocols with different combinations of b values were used. As recently shown, different combinations of b values have a direct impact on ADC values and even on the ability of DWI to distinguish between HPV-positive and HPV-negative HNSCC.[104,105] Nevertheless, the combination of precise morphologic MR imaging criteria with DWI and PET characteristics enables reliable distinction between edema, fibrosis, and recurrent/residual HNSCC on PET/DWIMR imaging.[6] Inflammatory edema can have a variable FDG uptake on PET images and variable contrast enhancement on MR imaging. On T2W images, poorly delineated areas with a high signal intensity are seen, and on DWI, there is no restricted diffusivity; therefore, ADC values are high (T2 shine through effect)[6,103,106] (**Fig. 14**). Fibrosis can display variable FDG uptake and variable contrast enhancement; however, a very low signal intensity on T2W images and a low ADC.[13,103] Because late fibrosis is mainly composed of densely packed collagen, ADCs tend to be low because of the T2 blackout effect (**Fig. 15**). Finally, recurrent HNSCC typically displays a strong FDG uptake, moderate contrast enhancement, an intermediate signal intensity on T2W images and restricted diffusivity[6] (**Figs. 16** and **17**). By

combining these criteria, we reported a high diagnostic performance with PET/DWIMR imaging for the detection of recurrent/residual disease after radiotherapy in a prospective study including 74 patients.[6] The standard of reference was histopathology of the resected specimen in 62% and a mean follow-up of 34 months in 38% of patients. Sensitivity, specificity, PPV, and NPV of PET/DWIMR imaging were 97%, 92%, 92.5%, and 97% per patient and 93.0%, 93.5%, 91%, and 95% per lesion, respectively. Agreement between imaging-based and pathologic T stage of resected tumors was excellent (kappa = 0.84, $P < .001$).

The interpretation of multiparametric data is challenging, especially if morphologic MR imaging, DWI, and PET findings are discrepant. On the one hand, this diagnostic uncertainty can lead to unnecessary biopsy in irradiated tissues; on the other hand, it can lead to delay in diagnosis if a "wait and see" policy is adopted. Our study may show a way to manage concordant/discordant readings as positive concordant results with PET, DWI, and MR imaging corresponded to recurrent tumors in 97.5% of cases and discordant results corresponded to benign lesions in 87% of cases, respectively[6] (**Fig. 18**). This approach could also be applied in indeterminate/suspicious FDG-PET/CT readings in which case a high ADC revealed by DWIMR imaging or the typical aspect of fibrosis on T2W and DWI images would lead to a wait and see policy instead of biopsy (**Fig. 19**). Moreover, based on a series of 69 HNSCC posttreatment patients, Ashour and colleagues have recently reported that the addition of DWI features and T2 signal to the American College of Radiology (ACR) Neck Imaging Reporting and Data System (NI-RADS) criteria for the primary tumor site enhanced specificity, sensitivity, PPV, NPV, and NI-RADS accuracy.[107]

Applying the NI-RADS criteria[16] to PET/MR imaging in a retrospective study including 46 patients, Patel and colleagues reported that PET/MR imaging scores showed a strong association with treatment failure for the primary site, neck lymph nodes, and combined sites, and the AUCs of PET/MR imaging scores versus treatment failure were 0.864 to 0.987, $P < .001$.[108] The investigators, therefore, concluded that PET/MR imaging has an excellent discriminatory performance for treatment outcomes of HNSCC when NI-RADS is applied.

An increasing number of studies using PET, DWI, DCE perfusion, and MR imaging parameters have recently investigated which imaging-based biomarkers could predict disease-free survival and overall survival in HNSCC patients.[109–112] A detailed discussion is beyond the scope of this article. Nevertheless, the published results suggest that models based on combined imaging biomarkers and clinical characteristics (eg, plasma EBV or HPV status) are very promising and may aid in planning the optimal personalized treatment strategy.

SUMMARY

Although the published research regarding the use of PET/MR imaging in HNSCC is relatively sparse, it seems that PET/MR imaging has at least a similar diagnostic performance as PET/CT for locoregional tumor staging with advantages in certain scenarios. Such scenarios include the assessment of tumor invasion in anatomic areas, which affect resectability, for example, the prevertebral space or PNS. As in most publications, the MR imaging part of PET/MR imaging has been mainly used for anatomic orientation, the full potential of PET/MR imaging has not been used, and only very few studies have incorporated multiparametric information so far. Nevertheless, multiparametric FDG PET/MR imaging with DWI has been shown to have a high diagnostic accuracy for the detection of residual/recurrent HNSCC after radiotherapy with an excellent agreement between imaging-based and pathologic T stage. FDG PET/MR imaging also has an excellent and similar diagnostic performance as FDG PET/CT for detecting distant metastases and distant second primary cancers in HNSCC patients. Imaging biomarkers derived from multiparametric PET/MR imaging with diffusion and perfusion sequences hold promise in predicting patient outcome and, therefore, in planning the optimal personalized treatment strategy. DL-based automatic tumor segmentation using PET data has become a reality, and PET/MR imaging may facilitate DL-based segmentation tasks incorporating multimodality information.

CLINICS CARE POINTS

- Both primary and recurrent head and neck squamous cell carcinoma (HNSCC) have characteristic PET/diffusion-weighted imaging (DWI) MR imaging features, which include the following: an intermediate signal intensity on T1W, T2W, or fat-saturated T2W sequences, and moderate enhancement after IV administration of contrast material; restricted diffusivity with apparent diffusion coefficient (ADC) values less than 1.2 to 1.3 $\times$ 10 to 3 mm^2/s; increased FDG uptake with SUVmax values most often greater than 3.
- MR imaging reliably detects perineural spread (PNS). Findings on MR imaging scans include

thickening, nodularity, nerve enhancement and fat pad obliteration, and denervation of muscles. PNS can be detected on FDG PET if tumors are FDG avid or in the presence of extensive PNS; nevertheless, correlation with MR imaging improves its assessment.

- The combination of morphologic MR imaging, DWI, and PET criteria allows improved detection of posttreatment recurrent HNSCC and distinction from inflammatory edema and fibrosis. Inflammatory edema can have variable FDG uptake and variable enhancement after IV administration of contrast material. On T2W images, inflammatory edema has a high signal intensity, and diffusivity is increased on DWI; therefore, ADC values are high. Fibrosis (scar tissue) can display variable FDG uptake and variable enhancement after IV administration of contrast material. Fibrosis has a very low signal intensity on T2W images and a low ADC.
- In HNSCC, both PET/MR imaging and PET/CT have a similar diagnostic performance for the detection of distant metastases and distant second primary cancers. Both benign and malignant lesions can show FDG uptake; however, SUVmean and SUVmax values are significantly higher in malignant lesions. As high FDG uptake can also cause false positive assessments, especially in the mediastinum, biopsy is necessary in certain situations.

DISCLOSURE

This review was part of a clinical research project funded by the Swiss National Science Foundation (SNSF) under grants No 320030_173091/1 and 320030_176052.

REFERENCES

1. Becker M, Zaidi H. Imaging in head and neck squamous cell carcinoma: the potential role of PET/MRI. Br J Radiol 2014;87(1036):20130677.
2. Zaidi H, Becker M. The promise of hybrid PET/MRI: Technical advances and clinical applications. IEEE Signal Proc Mag 2016;33(3):67–85.
3. Bülbül HM, Bülbül O, Sarıoğlu S, et al. Relationships Between DCE-MRI, DWI, and ^{18}F-FDG PET/CT Parameters with Tumor Grade and Stage in Patients with Head and Neck Squamous Cell Carcinoma. Mol Imaging Radionucl Ther 2021;30(3):177–86.
4. Zhang L, Song T, Meng Z, et al. Correlation between apparent diffusion coefficients and metabolic parameters in hypopharyngeal squamous cell carcinoma: A prospective study with integrated PET/MRI. Eur J Radiol 2020;129:109070.
5. Chan SC, Yeh CH, Ng SH, et al. Prospective Investigation of ^{18}FDG-PET/MRI with Intravoxel Incoherent Motion Diffusion-Weighted Imaging to Assess Survival in Patients with Oropharyngeal or Hypopharyngeal Carcinoma. Cancers 2022;14(24):6104.
6. Becker M, Varoquaux AD, Combescure C, et al. Local recurrence of squamous cell carcinoma of the head and neck after radio(chemo)therapy: Diagnostic performance of FDG-PET/MRI with diffusion-weighted sequences. Eur Radiol 2018; 28(2):651–63.
7. Varoquaux A, Rager O, Dulguerov P, et al. Diffusion-weighted and PET/MR Imaging after Radiation Therapy for Malignant Head and Neck Tumors. Radiographics 2015;35(5):1502–27.
8. Purohit BS, Ailianou A, Dulguerov N, et al. FDG-PET/CT pitfalls in oncological head and neck imaging. Insights Imaging 2014;5(5):585–602.
9. Albertson M, Chandra S, Sayed Z, et al. PET/CT Evaluation of Head and Neck Cancer of Unknown Primary. Semin Ultrasound CT MR 2019;40(5): 414–23.
10. Noij DP, Martens RM, Zwezerijnen B, et al. Diagnostic value of diffusion-weighted imaging and ^{18}F-FDG-PET/CT for the detection of unknown primary head and neck cancer in patients presenting with cervical metastasis. Eur J Radiol 2018;107: 20–5.
11. Johnson DE, Burtness B, Leemans CR, et al. Head and neck squamous cell carcinoma. Nat Rev Dis Primers 2020;6:92.
12. Pisani P, Airoldi M, Allais A, et al. Metastatic disease in head & neck oncology. Acta Otorhinolaryngol Ital 2020;40(SUPPL. 1):S1–86.
13. Becker M, De Vito C, Monnier Y. Imaging of laryngeal and hypopharyngeal cancer. Magn Reson Imag Clin N Am 2022;30(Issue 1):53–72.
14. Ng SP, Pollard C 3rd, Berends J, et al. Usefulness of surveillance imaging in patients with head and neck cancer who are treated with definitive radiotherapy. Cancer 2019;125(11):1823–9.
15. Galgano SJ, Marshall RV, Middlebrooks EH, et al. PET/MR Imaging in Head and Neck Cancer: Current Applications and Future Directions. Magn Reson Imaging Clin N Am 2018;26(1):167–78.
16. Mukherjee S, Fischbein NJ, Baugnon KL, et al. Contemporary Imaging and Reporting Strategies for Head and Neck Cancer: MRI, FDG PET/MRI, NI-RADS, and Carcinoma of Unknown Primary-*AJR* Expert Panel Narrative Review. AJR Am J Roentgenol 2023;220(2):160–72.
17. Eiber M, Souvatzoglou M, Pickhard A, et al. Simulation of a MR-PET protocol for staging of head-and-neck cancer including Dixon MR for attenuation correction. Eur J Radiol 2012;81:2658–65.
18. Vargas MI, Becker M, Garibotto V, et al. Approaches for the optimization of MR protocols in

clinical hybrid PET/MRI studies. Magma 2013;26: 57–69.
19. Varoquaux A, Rager O, Poncet A, et al. Detection and quantification of focal uptake in head and neck tumours: (18)F-FDG PET/MR versus PET/CT. Eur J Nucl Med Mol Imaging 2014;41(3):462–75.
20. von Schulthess GK, Kuhn FP, Kaufmann P, et al. Clinical positron emission tomography/magnetic resonance imaging applications. Semin Nucl Med 2013;43(1):3–10.
21. Queiroz MA, Huellner MW. PET/MR in cancers of the head and neck. Semin Nucl Med 2015;45(3): 248–65.
22. Platzek I. 18)F-Fluorodeoxyglucose PET/MR Imaging in Head and Neck Cancer. Pet Clin 2016; 11(4):375–86.
23. Huellner MW. PET/MR in Head and Neck Cancer - An Update. Semin Nucl Med 2021 Jan;51(1): 26–38.
24. Katirtzidou E, Rager O, Varoquaux AD, et al. Detection of distant metastases and distant second primary cancers in head and neck squamous cell carcinoma: comparison of [^{18}F]FDG PET/MRI and [^{18}F]FDG PET/CT. Insights Imaging 2022 Jul 28; 13(1):121.
25. Seifert R, Kersting D, Rischpler C, et al. Clinical Use of PET/MR in Oncology: An Update. Semin Nucl Med 2022 May;52(3):356–64.
26. Drzezga A, Souvatzoglou M, Eiber M, et al. First clinical experience with integrated whole-body PET/MR: comparison to PET/CT in patients with oncologic diagnoses. J Nucl Med 2012 Jun;53(6): 845–55.
27. Wiesmüller M, Quick HH, Navalpakkam B, et al. Comparison of lesion detection and quantitation of tracer uptake between PET from a simultaneously acquiring whole-body PET/MR hybrid scanner and PET from PET/CT. Eur J Nucl Med Mol Imaging 2013 Jan;40(1):12–21.
28. Bini J, Izquierdo-Garcia D, Mateo J, et al. Preclinical evaluation of MR attenuation correction versus CT attenuation correction on a sequential whole-body MR/PET scanner. Invest Radiol 2013 May; 48(5):313–22.
29. Arabi H, Rager O, Alem A, et al. Clinical assessment of MR-guided 3-class and 4-class attenuation correction in PET/MR. Mol Imaging Biol 2015;17(2): 264–76.
30. Varoquaux A, Rager O, Lovblad KO, et al. Functional imaging of head and neck squamous cell carcinoma with diffusion-weighted MRI and FDG PET/CT: quantitative analysis of ADC and SUV. Eur J Nucl Med Mol Imaging 2013 Jun;40(6): 842–52.
31. Freihat O, Zoltán T, Pinter T, et al. Correlation between Tissue Cellularity and Metabolism Represented by Diffusion-Weighted Imaging (DWI) and 18F-FDG PET/MRI in Head and Neck Cancer (HNC). Cancers 2022 Feb 8;14(3):847.
32. Fruehwald-Pallamar J, Czerny C, Mayerhoefer ME, et al. Functional imaging in head and neck squamous cell carcinoma: Correlation of PET/CT and diffusion-weighted imaging at 3 Tesla. Eur J Pediatr 2011;38:1009–19.
33. Min M, Lee MT, Lin P, et al. Assessment of serial multi-parametric functional MRI (diffusion-weighted imaging and R2*) with18F-FDG-PET in patients with head and neck cancer treated with radiation therapy. Br J Radiol 2016;89:20150530.
34. Rasmussen JH, Nørgaard M, Hansen AE, et al. Feasibility of Multiparametric Imaging with PET/MR in Head and Neck Squamous Cell Carcinoma. J Nucl Med 2017;58:69–74.
35. Covello M, Cavaliere C, Aiello M, et al. Simultaneous PET/MR head–neck cancer imaging: Preliminary clinical experience and multiparametric evaluation. Eur J Radiol 2015;84:1269–76.
36. Cheng Y, Bai L, Shang J, et al. Preliminary clinical results for PET/MR compared with PET/CT in patients with nasopharyngeal carcinoma. Oncol Rep 2020;43(1):177–87.
37. Nakajo M, Nakajo M, Kajiya Y, et al. FDG PET/CT and diffusion-weighted imaging of head and neck squamous cell carcinoma: Comparison of prognostic significance between primary tumour standardized uptake value and apparent diffusion coefficient. Clin Nucl Med 2012;37:475–80.
38. Han M, Kim SY, Lee SJ, et al. The Correlations Between MRI Perfusion, Diffusion Parameters, and 18F-FDG PET Metabolic Parameters in Primary Head-and-Neck Cancer. Medicine 2015;94:e2141.
39. Schaarschmidt BM, Heusch P, Buchbender C, et al. Locoregional tumour evaluation of squamous cell carcinoma in the head and neck area: a comparison between MRI, PET/CT and integrated PET/MRI. Eur J Nucl Med Mol Imaging 2016; 43(1):92–102.
40. Huang C, Song T, Mukherji SK, et al. Comparative Study Between Integrated Positron Emission Tomography/Magnetic Resonance and Positron Emission Tomography/Computed Tomography in the T and N Staging of Hypopharyngeal Cancer: An Initial Result. J Comput Assist Tomogr 2020; 44(4):540–5.
41. Sekine T a, de Galiza Barbosa F, Kuhn FP, et al. PET+MR versus PET/CT in the initial staging of head and neck cancer, using a trimodality PET/CT+MR system. Clin Imaging 2017;42:232–9.
42. Samolyk-Kogaczewska N, Sierko E, Dziemianczyk-Pakiela D, et al. Usefulness of Hybrid PET/MRI in Clinical Evaluation of Head and Neck Cancer Patients. Cancers 2020;12(2):511.
43. Flygare L, Erdogan ST, Söderkvist K. PET/MR versus PET/CT for locoregional staging of oropharyngeal

squamous cell cancer. Acta Radiol 2023;64(5):1865–72.
44. Chan SC, Yeh CH, Yen TC, et al. Clinical utility of simultaneous whole-body ^{18}F-FDG PET/MRI as a single-step imaging modality in the staging of primary nasopharyngeal carcinoma. Eur J Nucl Med Mol Imaging 2018;45(8):1297–308.
45. Kuhn FP, Hüllner M, Mader CE, et al. Contrast-enhanced PET/MR imaging versus contrast-enhanced PET/CT in head and neck cancer: how much MR information is needed? J Nucl Med 2014;55(4):551–8.
46. Meerwein CM, Pizzuto DA, Vital D, et al. Use of MRI and FDG-PET/CT to predict fixation of advanced hypopharyngeal squamous cell carcinoma to prevertebral space. Head Neck 2019;41(2):503–10.
47. Sekine T b, Barbosa FG, Delso G, et al. Local resectability assessment of head and neck cancer: Positron emission tomography/MRI versus positron emission tomography/CT. Head Neck 2017;39(8):1550–8.
48. Medvedev O, Hedesiu M, Ciurea A, et al. Perineural spread in head and neck malignancies: imaging findings - an updated literature review. Bosn J Basic Med Sci 2022;22(1):22–38.
49. Lee H, Lazor JW, Assadsangabi R, et al. An Imager's Guide to Perineural Tumor Spread in Head and Neck Cancers: Radiologic Footprints on ^{18}F-FDG PET, with CT and MRI Correlates. J Nucl Med 2019;60(3):304–11.
50. Abdelaziz TT, Abdel Razek AAK. Magnetic Resonance Imaging of Perineural Spread of Head and Neck Cancer. Magn Reson Imaging Clin N Am 2022;30(1):95–108.
51. Cao C, Xu Y, Huang S, et al. Locoregional Extension Patterns of Nasopharyngeal Carcinoma Detected by FDG PET/MR. Front Oncol 2021;11:763114.
52. Nie X, Zhou J, Zeng J, et al. Does PET scan have any role in the diagnosis of perineural spread associated with the head and neck tumors? Adv Clin Exp Med 2022;31(8):827–35.
53. Audet N, Beasley NJ, MacMillan C, et al. Lymphatic vessel density, nodal metastases, and prognosis in patients with head and neck cancer. Arch Otolaryngol Head Neck Surg 2005;131:1065–70.
54. Platzek I, Beuthien-Baumann B, Schneider M, et al. FDG PET/MR for lymph node staging in head and neck cancer. Eur J Radiol 2014;83(7):1163–8.
55. Cebeci S, Aydos U, Yeniceri A, et al. Diagnostic performance of FDG PET/MRI for cervical lymph node metastasis in patients with clinically N0 head and neck cancer. Eur Rev Med Pharmacol Sci 2023;27(10):4528–35.
56. Crimì F, Borsetto D, Stramare R, et al. [^{18}F]FDG PET/MRI versus contrast-enhanced MRI in detecting regional HNSCC metastases. Ann Nucl Med 2021;35(2):260–9.
57. Mundada P, Varoquaux AD, Lenoir V, et al. Utility of MRI with morphologic and diffusion weighted imaging in the detection of post-treatment nodal disease in head and neck squamous cell carcinoma. Eur J Radiol 2018;101:162–9.
58. Vandecaveye V, De Keyzer F, Vander Poorten V, et al. Head and neck squamous cell carcinoma: value of diffusion-weighted MR imaging for nodal staging. Radiology 2009;251(1):134–46.
59. de Bondt RB, Hoeberigs MC, Nelemans PJ, et al. Diagnostic accuracy and additional value of diffusion-weighted imaging for discrimination of malignant cervical lymph nodes in head and neck squamous cell carcinoma. Neuroradiology 2009;51(3):183–92.
60. Dirix P, Vandecaveye V, De Keyzer F, et al. Diffusion-weighted MRI for nodal staging of head and neck squamous cell carcinoma: impact on radiotherapy planning. Int J Radiat Oncol Biol Phys 2010 Mar 1;76(3):761–6.
61. Driessen JP, van Kempen PM, van der Heijden GJ, et al. Diffusion-weighted imaging in head and neck squamous cell carcinomas: a systematic review. Head Neck 2015;37(3):440–8.
62. Belfiore MP, Gallo L, Reginelli A, et al. Quantitative Evaluation of the Lymph Node Metastases in the Head and Neck Malignancies Using Diffusion-Weighted Imaging and Apparent Diffusion Coefficient Mapping: A Bicentric Study. Magnetochemistry 2023;9(5):124.
63. Chen J, Hagiwara M, Givi B, et al. Assessment of metastatic lymph nodes in head and neck squamous cell carcinomas using simultaneous ^{18}F-FDG-PET and MRI. Sci Rep 2020;10(1):20764.
64. Freihat O, Pinter T, Kedves A, et al. Diffusion-Weighted Imaging (DWI) derived from PET/MRI for lymph node assessment in patients with Head and Neck Squamous Cell Carcinoma (HNSCC). Cancer Imag 2020;20(1):56.
65. Gao S, Li S, Yang X, et al. 18FDG PET-CT for distant metastases in patients with recurrent head and neck cancer after definitive treatment. A meta-analysis. Oral Oncol 2014;50(3):163–7.
66. Yeh CH, Chan SC, Lin CY, et al. Comparison of ^{18}F-FDG PET/MRI, MRI, and ^{18}F-FDG PET/CT for the detection of synchronous cancers and distant metastases in patients with oropharyngeal and hypopharyngeal squamous cell carcinoma. Eur J Nucl Med Mol Imaging 2020;47(1):94–104.
67. de Bree R, Senft A, Coca-Pelaz A, et al. Detection of Distant Metastases in Head and Neck Cancer: Changing Landscape. Adv Ther 2018;35(2):161–72.
68. Chandarana H, Heacock L, Rakheja R, et al. Pulmonary nodules in patients with primary malignancy: comparison of hybrid PET/MR and PET/CT imaging. Radiology 2013;268(3):874–81.

69. Lee KH, Park CM, Lee SM, et al. Pulmonary Nodule Detection in Patients with a Primary Malignancy Using Hybrid PET/MRI: Is There Value in Adding Contrast-Enhanced MR Imaging? PLoS One 2015;10(6):e0129660.
70. Zhang C, Liang Z, Liu W, et al. Comparison of whole-body 18F-FDG PET/CT and PET/MRI for distant metastases in patients with malignant tumors: a meta-analysis. BMC Cancer 2023;23(1):37.
71. Botsikas D, Bagetakos I, Picarra M, et al. What is the diagnostic performance of 18-FDG-PET/MR compared to PET/CT for the N- and M- staging of breast cancer? Eur Radiol 2019;29(4):1787–98.
72. Schwenzer NF, Schraml C, Müller M, et al. Pulmonary lesion assessment: comparison of whole-body hybrid MR/PET and PET/CT imaging–pilot study. Radiology 2012;264(2):551–8.
73. van Weert S, Hendrickx JJ, Leemans CR. Carcinoma of Unknown Primary: Diagnostics and the Potential of Transoral Surgery. In: Vermorken JB, Budach V, Leemans CR, et al, editors. Critical issues in head and neck oncology. Cham: Springer; 2023.
74. Brierley JD, Gospodarowicz MK, Wittekind C, et al, editors. UICC TNM classification of malignant tumours. 8th edition. Hoboken, New Jersey: Wiley Blackwell: Union for International Cancer Control; 2017.
75. Kalavacherla S, Sanghvi P, Lin GY, et al. Updates in the management of unknown primary of the head and neck. Front Oncol 2022;12:991838.
76. Chen B, Zhang H, Liu D, et al. Diagnostic performance of 18F-FDG PET/CT for the detection of occult primary tumors in squamous cell carcinoma of unknown primary in the head and neck: a single-center retrospective study. Nucl Med Commun 2021;42(5):523–7.
77. Rudmik L, Lau HY, Matthews TW, et al. Clinical utility of PET/CT in the evaluation of head and neck squamous cell carcinoma with an unknown primary: a prospective clinical trial. Head Neck 2011;33:935–40.
78. Ruhlmann V, Ruhlmann M, Bellendorf A, et al. Hybrid imaging for detection of carcinoma of unknown primary: a preliminary comparison trial of whole-body PET/MRI versus PET/CT. Eur J Radiol 2016;85(11):1941–7.
79. Decazes P, Hinault P, Veresezan O, et al. Trimodality PET/CT/MRI and Radiotherapy: A Mini-Review. Front Oncol 2021;10:614008.
80. Terzidis E, Friborg J, Vogelius IR, et al. Tumor volume definitions in head and neck squamous cell carcinoma - Comparing PET/MRI and histopathology. Radiother Oncol 2023;180:109484.
81. Adjogatse D, Petkar I, Reis Ferreira M, et al. The Impact of Interactive MRI-Based Radiologist Review on Radiotherapy Target Volume Delineation in Head and Neck Cancer. AJNR Am J Neuroradiol 2023;44(2):192–8.
82. Shiri I, Vafaei Sadr A, Amini M, et al. Decentralized Distributed Multi-institutional PET Image Segmentation Using a Federated Deep Learning Framework. Clin Nucl Med 2022;47(7):606–17.
83. Arslan S, Abakay CD, Sen F, et al. Role of PET/CT in treatment planning for head and neck cancer patients undergoing definitive radiotherapy. Asian Pac J Cancer Prev 2014;15(24):10899–903.
84. Newbold K, Powell C. PET/CT in Radiotherapy Planning for Head and Neck Cancer. Front Oncol 2012;2:189.
85. Nicolay NH, Wiedenmann N, Mix M, et al. Correlative analyses between tissue-based hypoxia biomarkers and hypoxia PET imaging in head and neck cancer patients during radiochemotherapy-results from a prospective trial. Eur J Nucl Med Mol Imaging 2020;47(5):1046–55.
86. Santos Armentia E, Martín Noguerol T, Suárez Vega V. Advanced magnetic resonance imaging techniques for tumors of the head and neck. Radiologia (Engl Ed) 2019;61(3):191–203.
87. Winter RM, Leibfarth S, Schmidt H, et al. Assessment of image quality of a radiotherapy-specific hardware solution for PET/MRI in head and neck cancer patients. Radiother Oncol 2018;128(3):485–91.
88. Wang K, Mullins BT, Falchook AD, et al. Evaluation of PET/MRI for Tumor Volume Delineation for Head and Neck Cancer. Front Oncol 2017;7:8.
89. Samołyk-Kogaczewska N, Sierko E, Zuzda K, et al. PET/MRI-guided GTV delineation during radiotherapy planning in patients with squamous cell carcinoma of the tongue. Strahlenther Onkol 2019;195(9):780–91.
90. Bird D, Scarsbrook AF, Sykes J, et al. Multimodality imaging with CT, MR and FDG-PET for radiotherapy target volume delineation in oropharyngeal squamous cell carcinoma. BMC Cancer 2015;15:844.
91. Braunstein S, Glastonbury CM, Chen J, et al. Impact of Neuroradiology-Based Peer Review on Head and Neck Radiotherapy Target Delineation. AJNR Am J Neuroradiol 2017 Jan;38(1):146–53.
92. Chiu K, Hoskin P, Gupta A, et al. The quantitative impact of joint peer review with a specialist radiologist in head and neck cancer radiotherapy planning. Br J Radiol 2022;95(1130):20211219.
93. Illimoottil M, Ginat D. Recent Advances in Deep Learning and Medical Imaging for Head and Neck Cancer Treatment: MRI, CT, and PET Scans. Cancers 2023;15(13):3267.
94. Arabi H, Shiri I, Jenabi E, et al. Deep Learning-based Automated Delineation of Head and Neck Malignant Lesions from PET Images. IEEE 2020. https://doi.org/10.1109/NSS/MIC42677.2020.9507977.

95. Shiri I, Arabi H, Sanaat A, et al. Fully Automated Gross Tumor Volume Delineation from PET in Head and Neck Cancer using deep learning algorithms. Clin Nucl Med 2021;46(11):872–83.
96. Shiri I, Amini M, Yousefirizi F, et al. Information fusion for fully automated segmentation of head and neck tumors from PET and CT images. Med Phys 2023. https://doi.org/10.1002/mp.16615.
97. Kaissis GA, Makowski MR, Ruckert D, et al. Secure, privacy-preserving and federated machine learning in medical imaging. Nat Mach Intell 2020; 2:305–11.
98. Sheikhbahaei S, Taghipour M, Ahmad R, et al. Diagnostic Accuracy of Follow-Up FDG PET or PET/CT in Patients With Head and Neck Cancer After Definitive Treatment: A Systematic Review and Meta-Analysis. AJR Am J Roentgenol 2015; 205(3):629–39.
99. Cheung PK, Chin RY, Eslick GD. Detecting Residual/Recurrent Head Neck Squamous Cell Carcinomas Using PET or PET/CT: Systematic Review and Meta-analysis. Otolaryngol Head Neck Surg 2016;154(3):421–32.
100. Gupta T, Master Z, Kannan S, et al. Diagnostic performance of post-treatment FDG PET or FDG PET/CT imaging in head and neck cancer: a systematic review and meta-analysis. Eur J Nucl Med Mol Imaging 2011;38:2083–95.
101. Abdel Razek AA, Kandeel AY, Soliman N, et al. Role of diffusion-weighted echo-planar MR imaging in differentiation of residual or recurrent head and neck tumors and posttreatment changes. AJNR Am J Neuroradiol 2007;28(6):1146–52.
102. Vandecaveye V, De Keyzer F, Nuyts S, et al. Detection of head and neck squamous cell carcinoma with diffusion weighted MRI after (chemo)radiotherapy: correlation between radiologic and histopathologic findings. Int J Radiat Oncol Biol Phys 2007;67(4):960–71.
103. Ailianou A, Mundada P, De Perrot T, et al. MRI with DWI for the Detection of Posttreatment Head and Neck Squamous Cell Carcinoma: Why Morphologic MRI Criteria Matter. AJNR Am J Neuroradiol 2018 Apr;39(4):748–55.
104. Lenoir V, Delattre BMA, M'RaD Y, et al. Diffusion-Weighted Imaging to Assess HPV-Positive versus HPV-Negative Oropharyngeal Squamous Cell Carcinoma: The Importance of b-Values. AJNR Am J Neuroradiol 2022;43(6):905–12.
105. de Perrot T, Lenoir V, Domingo Ayllón M, et al. Apparent Diffusion Coefficient Histograms of Human Papillomavirus-Positive and Human Papillomavirus-Negative Head and Neck Squamous Cell Carcinoma: Assessment of Tumor Heterogeneity and Comparison with Histopathology. AJNR Am J Neuroradiol 2017;38(11):2153–60.
106. King AD, Keung CK, Yu KH, et al. T2-weighted MR imaging early after chemoradiotherapy to evaluate treatment response in head and neck squamous cell carcinoma. AJNR Am J Neuroradiol 2013;34: 1237–41.
107. Ashour MM, Darwish EAF, Fahiem RM, et al. MRI Posttreatment Surveillance for Head and Neck Squamous Cell Carcinoma: Proposed MR NI-RADS Criteria. AJNR Am J Neuroradiol 2021; 42(6):1123–9.
108. Patel LD, Bridgham K, Ciriello J, et al. PET/MR Imaging in Evaluating Treatment Failure of Head and Neck Malignancies: A Neck Imaging Reporting and Data System-Based Study. AJNR Am J Neuroradiol 2022;43(3):435–41.
109. Martens RM, Noij DP, Koopman T, et al. Predictive value of quantitative diffusion-weighted imaging and 18-F-FDG-PET in head and neck squamous cell carcinoma treated by (chemo)radiotherapy. Eur J Radiol 2019;113:39–50.
110. Pace L, Nicolai E, Cavaliere C, et al. Prognostic value of 18F-FDG PET/MRI in patients with advanced oropharyngeal and hypopharyngeal squamous cell carcinoma. Ann Nucl Med 2021 Apr;35(4):479–84.
111. Chan SC, Yeh CH, Chang JT, et al. Combing MRI Perfusion and ^{18}F-FDG PET/CT Metabolic Biomarkers Helps Predict Survival in Advanced Nasopharyngeal Carcinoma: A Prospective Multimodal Imaging Study. Cancers 2021;13(7):1550.
112. Connor S, Sit C, Anjari M, et al. The ability of post-chemoradiotherapy DWI ADC_{mean} and ^{18}F-FDG SUV_{max} to predict treatment outcomes in head and neck cancer: impact of human papilloma virus oropharyngeal cancer status. J Cancer Res Clin Oncol 2021;147(8):2323–36.